APPLIED RESEARCH LABORATORIES
THE UNIVERSITY OF TEXAS AT AUSTIN

ARL-TR-70-43
17 December 1970

Copy No. 46

SKIN FRICTION AND HEAT TRANSFER IN TURBULENT BOUNDARY LAYERS AS INFLUENCED BY ROUGHNESS

Part I, Final Report Under APL/JHU Subcontract 271734, Task B
1 March 1968 - 31 December 1970

Milton J. Thompson

NAVAL AIR SYSTEMS COMMAND
Under APL/JHU Subcontract 271734, Task B

Approved for public release;
distribution unlimited.

96

UNCLASSIFIED

Security Classification

DOCUMENT CONTROL DATA - R & D

(Security classification of title, body of abstract and indexing annotation must be entered when the overall report is classified)

1. ORIGINATING ACTIVITY (Corporate author)	2a. REPORT SECURITY CLASSIFICATION
Applied Research Laboratories The University of Texas at Austin Austin, Texas 78712	UNCLASSIFIED
	2b. GROUP ---

3. REPORT TITLE

SKIN FRICTION AND HEAT TRANSFER IN TURBULENT BOUNDARY LAYERS AS INFLUENCED BY ROUGHNESS, PART I, FINAL REPORT UNDER APL/JHU SUBCONTRACT 271734, TASK B

4. DESCRIPTIVE NOTES (Type of report and inclusive dates)

Technical Report 1 March 1968 - 31 December 1970

5. AUTHOR(S) (First name, middle initial, last name)

Milton J. Thompson

6. REPORT DATE	7a. TOTAL NO. OF PAGES	7b. NO. OF REFS
17 December 1970	98	32

8a. CONTRACT OR GRANT NO.	9a. ORIGINATOR'S REPORT NUMBER(S)
APL/JHU Subcontract 271734 b. PROJECT NO. Task B c. d.	ARL-TR-70-43
	9b. OTHER REPORT NO(S) (Any other numbers that may be assigned this report) ---

10. DISTRIBUTION STATEMENT

Approved for public release; distribution unlimited.

11. SUPPLEMENTARY NOTES	12. SPONSORING MILITARY ACTIVITY
---	Naval Air Systems Command Department of the Navy Washington, D. C. 20360

13. ABSTRACT

This report provides a summary of ~~an extended program of~~ theoretical and experimental research on turbulent boundary layers under supersonic free stream conditions. The program ~~began with~~ investigations of boundary layer behavior at various Mach Numbers for smooth, adiabatic surfaces, ~~later~~ phases involved the addition of various types of surface roughness, ~~with consideration in the final aspects being~~ given ~~to~~ the combined effects of roughness and heat transfer. The experimental program involved ~~the utilization of~~ velocity profile measurements and the momentum deficit method of calculating skin friction, the application of both the floating element skin friction balance and the Preston tube for determinations of local shear stress values, and the utilization of plug-type calorimeters for determinations of heat transfer rates. (U)

DD FORM 1 NOV 68 1473 (PAGE 1)

S/N 0101-807-6801

UNCLASSIFIED

Security Classification

14 KEY WORDS	LINK A		LINK B		LINK C	
	ROLE	WT	ROLE	WT	ROLE	WT
Compressible Flow						
Turbulent Boundary Layers						
Skin Friction						
Aerodynamic Heating						
Roughness						

ARL-TR-70-43
17 December 1970

SKIN FRICTION AND HEAT TRANSFER IN TURBULENT BOUNDARY LAYERS AS INFLUENCED BY ROUGHNESS

Part I, Final Report Under APL/JHU Subcontract 271734, Task B
1 March 1968 - 31 December 1970

Milton J. Thompson

NAVAL AIR SYSTEMS COMMAND
Under APL/JHU Subcontract 271734, Task B

This work has been sponsored by the Naval Air Systems Command, under Subcontract 271734 with the Applied Physics Laboratory of The Johns Hopkins University

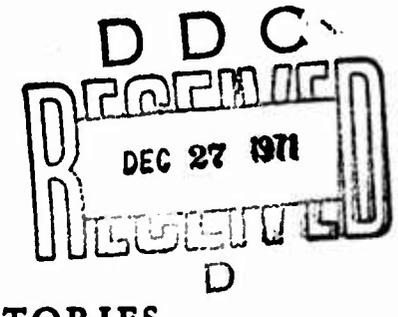

APPLIED RESEARCH LABORATORIES
THE UNIVERSITY OF TEXAS AT AUSTIN
AUSTIN, TEXAS 78712

ABSTRACT

This report provides a summary of an extended program of theoretical and experimental research on turbulent boundary layers under supersonic free stream conditions. The program began with investigations of boundary layer behavior at various Mach Numbers for smooth, adiabatic surfaces. Later phases involved the addition of various types of surface roughness, with consideration in the final aspects being given to the combined effects of roughness and heat transfer. The experimental program involved the utilization of velocity profile measurements and the momentum deficit method of calculating skin friction, the application of both the floating element skin friction balance and the Preston tube for determinations of local shear stress values, and the utilization of plug-type calorimeters for determinations of heat transfer rates.

PREFACE

The ARL program of boundary layer research was initiated in 1947 in order to provide basic technical data on the flow characteristics of turbulent boundary layers under supersonic free stream conditions. The immediate application of such information was contemplated as related to aerodynamic design problems of guided missiles and high speed aircraft, both of which were beginning to attain operational values of flight Mach Numbers greater than unity. Emphasis was placed on the turbulent boundary layer because it was felt that surface conditions on a typical flight vehicle would be most likely to result in such situations, rather than in the laminar type of flow usually related to lower ranges of the flight Reynolds Number and to extremely small values of surface roughness.

The ARL aerodynamic research program as a whole developed out of the writer's participating during 1945 in the Bumblebee program of the Applied Physics Laboratory of The Johns Hopkins University. After completion of that assignment and return to The University of Texas at Austin, arrangements were made for a continuation of certain phases of the Bumblebee program at the latter institution. Such activities were initially conducted under the aegis of an interdisciplinary activity originally designated as the Defense Research Laboratory and later renamed Applied Research Laboratories, its present title.

Support for these DRL/ARL research activities was provided initially by the Navy Bureau of Ordnance through a series of research

contracts which were monitored by the Applied Physics Laboratory. A later reorganization of the Navy Department resulted in a transfer of responsibility for these programs to the Naval Air Systems Command, with technical responsibility continuing in the hands of APL/JHU. Significant contributions were also made by the Air Force Office of Aerospace Research and other Air Force technical divisions, particularly in the development of a significant supersonic wind tunnel facility that made it possible to conduct experimental investigations directly at the University.

In addition to providing useful information for the aerodynamic design problems of high speed flight vehicles, the research programs enabled engineering faculty members to participate actively in work of current and future technical importance. At the same time a substantial number of graduate students in engineering were employed as research engineers and assistants, with arrangements being made which enabled them to use the results of their studies as the basis for master's theses and doctoral dissertations. Many of these individuals have now moved on to higher level positions in education, industrial organizations, or research and development laboratories, where they continue to make substantial contributions to technology.

In view of the large number of individuals involved in all aspects of this program, it is impossible to acknowledge their contributions on an individual basis. They can be recognized only as members of the various participating groups involved in the support of the program, including the technical divisions of the Navy Department, The Johns Hopkins Applied Physics Laboratory, and the Air Force Office of Aerospace Research. The opportunity to participate in the exchange of information resulting from membership in the technical panels of the Bureau of Weapons Advisory Committee on Aeroballistics and the Navy Aeroballistics Advisory Committee

was of inestimable value. Recognition of the contributions of individual research workers at The University of Texas at Austin is given by listing of the technical reports for which they were responsible.

TABLE OF CONTENTS

TABLE OF CONTENTS (Cont'd)

NOMENCLATURE

a	- constant in roughness function for flat plates
b	- constant in roughness function for flat plates
A	- constant in "law of the wall" equation
A_r	- coefficient in "law of the wall" equation for rough plates
B	- constant in "law of the wall" equation
B_r	- coefficient in "law of the wall" equation for rough plates
B'_r	- coefficient in "law of the wall" equation for rough plates
c	- constant in Harkness's cubic temperature function
c_f	- local skin friction coefficient
C	- constant in velocity defect law
C'	- constant in "law of the wake" equation
C_F	- mean skin friction coefficient for flat plates
C_{F_*}	- value of C_F based on wall conditions
C_p	- specific heat at constant pressure
d	- diameter of Preston tube
d_{cr}	- limiting value of Preston tube diameter
D_f	- frictional force on flat plate
e	- base of natural or Napierian logarithms
E	- Eckert Number = $2(T_s-T_1)/(T_w-T_1)$
$f(\eta)$	- Coles' function in "law of the wall" equation
$f_1(\eta)$	- "law of the wall" value of $f(\eta)$
$f_2(\eta)$	- "law of the wake" value of $f(\eta)$
$f(\eta_r)$	- roughness function
$F(y/\delta)$	- velocity defect law function
h	- heat transfer coefficient
k	- proportionality coefficient in mixing length relation
k_{adm}	- admissible sand grain roughness diameter
k_r	- mean roughness diameter or height
k_s	- average sand grain roughness diameter
K	- constant in transition equation for C_F

K' - constant in "law of the wake" equation

ℓ - mixing length

l - plate length, measured from leading edge

m - Mach Number function = $(\gamma-1)M_1^2/2$

M - Mach Number at any point in flow

M_1 - Mach Number at outer edge of boundary layer

N - Nusselt Number = $h\ell/\lambda$

p - Reynolds Analogy factor

P - Prandtl Number = $\mu C_p/\lambda$

P_w - Prandtl Number at wall

$P_{w_{ins}}$ - Prandtl Number at insulated wall

q - heat transfer rate

r - pipe radius

r - temperature recovery factor

R - Reynolds Number = $\rho u\ell/\mu$

R_s - Reynolds Number at edge of laminar sublayer

R_* - Reynolds Number based on wall conditions

s - value of friction-distance parameter at edge of laminar sublayer

s_o - value of s at edge of laminar sublayer for insulated plate

S - Stanton Number = $h/\rho C_p u_1$

t - wall thickness for Preston tube

t - temperature function

t' - temperature function

T - absolute temperature

T_1 - temperature at outer edge of boundary layer

T_s - stagnation temperature

T_w - wall temperature

$T_{w_{ad}}$ - adiabatic wall temperature

u - velocity parallel to wall surface at any point within boundary layer

u_1 - value of u at outer edge of boundary layer

u_w - wall velocity, value of u at outer edge of laminar sublayer

u^* - friction velocity

$w(y/\ )$ - Coles' wake function

x - distance along plate surface measured from leading edge

X - function of Mach Number and skin friction coefficient

X' - function of Mach Number

y - distance across boundary layer measured from wall

Y - function of Mach Number and skin friction coefficient

Y' - function of Mach Number

Greek Symbols

β - exponent in "law of the wall" equation for compressible flow

γ - ratio of specific heats at constant pressure and constant volume

δ - boundary layer thickness

δ_2 - momentum thickness

δ_s - laminar sublayer thickness

λ - function of Mach Number and temperature ratio

λ - coefficient of thermal conductivity

μ - absolute viscosity of fluid

μ_1 - value of μ at outer edge of boundary layer

ν - kinematic viscosity of fluid

ν_1 - value of ν at outer edge of boundary layer

ν_w - value of ν at wall

Π - wake factor in Coles' "law of the wake"

ρ - mass density of fluid

σ - function of Mach Number

τ - shear stress

τ_o - shear stress at wall

φ - ratio of flow velocity to friction velocity = u/u^*

φ_1 - value of φ at outer edge of boundary layer

Ψ - function of σ and λ

ω - exponent in viscosity-temperature relation

Subscripts

1 - outer edge of boundary layer

o - wall conditions

s - outer edge of laminar sublayer

w - wall conditions

I. INTRODUCTION

This report presents a summary of research on turbulent boundary layers carried on over an extended period at the Applied Research Laboratories of The University of Texas at Austin. The work was supported initially by the Navy Bureau of Ordnance, and later by the Bureau of Weapons and the Air Systems Command, through a series of contracts with the Navy Department and more recently through subcontracts with the Applied Physics Laboratory of The Johns Hopkins University. Current activities are covered by APL/JHU Subcontract 271734.

In its early stages the research program was concerned with the determination of skin friction and boundary layer characteristics on a smooth flat plate. The experimental conditions selected for study were supersonic free stream velocities and adiabatic conditions insofar as heat transfer was concerned, the primary objective being to provide quantitative data on skin friction suitable for application to missile design problems over a moderate range of Mach Numbers. Turbulent flow conditions were chosen because it was felt, at that time at least, that the boundary layer flow on any operational vehicle would probably be of this character. Heat transfer effects were omitted from these early studies in order to provide a relatively simple approach to these problems. The initial phase of the test program was conducted in the supersonic wind tunnel of the Ordnance Aerophysics Laboratory at Daingerfield, a facility which made it possible to achieve a fairly high range of Reynolds Numbers as well as a modest range of low supersonic Mach Numbers. In 1957 the OAL wind tunnel was decommissioned and all testing was transferred to a

new facility developed at ARL with support from the Air Force Office of Aerospace Research. The ARL tunnel has a substantially smaller test section, 6 in. by 7 in., as compared to the 19 in. by 22 in. OAL tunnel, but the ARL tunnel does cover a wider range of Mach Numbers, i.e., from 2.00 to 5.00, approximately.

During the period of operation of the OAL tunnel, the research program was extended by the introduction of roughness effects, initially of a uniformly distributed character, and later in the form of transverse Veegrooves. Considerable attention was also devoted to the development of various types of instrumentation for the measurement of local shear stress. The initial smooth plate work had been accomplished by the use of a Pitot probe which traversed the boundary layer and provided a means of determining the mean skin friction up to the measuring station by a momentum deficit calculation. Early analytical studies of turbulent boundary layers brought forth the significance of local shear stress and its relation to the velocity distribution. This concept led to the development of a floating element type of balance, capable of measuring the shear force on a small disk set flush with the main boundary. The Pitot probe method was also extended to include Preston's technique of local shear determination by means of a tube resting directly on the plate surface. Correlations between these different methods were the subject of extended study.

In the development of the ARL wind tunnel, one of the initial design considerations involved the inclusion of an air preheating unit, primarily as a means of preventing condensation in the flow passing through the test section. The requirement for such a heater then led to an extension of the capacity of the unit, so as to make possible the execution of boundary layer tests with heat transfer for a modest range of heat transfer rates. In some cases

these rates were extended by internal cooling of the models being tested. The heat transfer tests were conducted both on a smooth plate and on roughened plates.

II. THEORETICAL BACKGROUND FOR INCOMPRESSIBLE FLOW

In order to fully understand the details of the experimental programs and the nature of the results obtained, it is necessary to provide a brief outline of basic boundary layer theory. The ARL program, with a few exceptions which will be mentioned later, did not include extensive analytical treatments of boundary layer flows, but rather utilized existing methods for this purpose.

Although many refinements have been introduced in boundary layer analysis, the most successful theoretical work still remains the mixing length theory, initiated by Prandtl, and later extended by Von Kármán. The basic physical assumptions concerning the flow are well described in any of the numerous treatises on fluid mechanics, with the work of Schlichting [Ref. (1)] representing one of the most comprehensive. The starting point of the analysis is the differential equation for the shear stress at any point in the boundary layer, which Prandtl derived in the form

$$\tau = -\rho \ell^2 (du/dy)^2 \quad . \tag{1}$$

This relation is based on the concept that momentum is transferred from one layer of fluid to another, there being a gradual retardation in the flow velocity as the boundary surface is approached. This basic equation has been used in studies of pipe flow and for boundary layer flows on flat plates and curved walls, the latter case involving a longitudinal pressure gradient.

In order to carry out the integration of Eq. (1), it is necessary to have available two additional pieces of information. One of these is the variation in shear stress across the boundary layer, that is, τ as a function of y, while the other is the value of the mixing length term ℓ. Prandtl reduced the problem to a relatively simple form by assuming that in the immediate vicinity of the boundary the shear stress is constant and equal to the value at the wall. His value of the mixing length factor was based on experiments made by Nikuradse on flow in smooth pipes which showed a pseudoparabolic variation in ℓ with y, reaching a maximum at the center of the pipe. Again, focusing his attention on the wall region, Prandtl used an approximate relation of the form

$$\ell \cong ky \quad , \tag{2}$$

where $k = 0.4$ is the slope of the curve of ℓ/r as a function of y/r at $y/r = 0$. The alternative assumption introduced by Von Kármán regarding the mixing length term is based on considerations of mechanical similitude of the turbulent flow pattern from one point to another. This leads to the relation

$$\ell = k(du/dy)/(d^2u/dy^2) \quad . \tag{3}$$

When either of the values of ℓ are introduced in Eq. (1), along with the constant shear stress assumption, the result in integrated form is obtained by introducing boundary conditions corresponding to the edge of a laminar sublayer between the body surface and the primary turbulent portion of the boundary layer. This assumption may be expressed in the form

$$yu^*/\nu_w = \delta_s u^*/\nu_w = s \quad , \tag{4}$$

in which ν_w is the kinematic viscosity at the wall, $u^* = \sqrt{\tau_o/\rho}$ is the so-called friction velocity, and the entire quantity in Eq. (4) is Prandtl's friction-distance parameter. Since yu^*/ν_w is a sort of Reynolds Number, it is assumed that its value s at $y = \delta_s$ is a critical value corresponding to the transition from the laminar flow in the sublayer to the turbulent flow outside it. Experimental evidence indicates that $s \cong 11.6$.

2.1 Development of the Law of the Wall

Before carrying out the integration of Eq. (1), it is convenient to introduce the nondimensional ratios

$$\varphi = u/u^* \quad \text{and} \quad \eta = yu^*/\nu_w \quad . \tag{5}$$

The integration of Eq. (1) with either Eq. (2) or (3) for ℓ then gives a result in the form

$$\varphi = A \log_{10}\eta + B \quad , \tag{6}$$

where the constants depend on the values assumed for k and s. In the case of an incompressible flow without heat transfer, the integration yields a result in the form

$$\varphi = \frac{1}{k}\left[\ell n\eta + \ell n\left(\frac{e^{ks}}{s}\right)\right] \quad . \tag{7}$$

This result involves the assumption that the velocity distribution within the laminar sublayer is linear, that is

$$u = u_w y/\delta_s \quad , \tag{8}$$

u_w being the so-called wall velocity or value of u at the outer edge of the sublayer. The shear stress within the sublayer is then given as

$$\tau_o = u\left(\frac{du}{dy}\right)_{y=0} = \frac{\mu u_w}{\delta_s} \quad , \tag{9}$$

or, after eliminating the wall velocity and replacing $\sqrt{\tau_o/\rho}$ by u*, which is the friction velocity, the sublayer velocity distribution is given as

$$\frac{u}{u^*} = \frac{u^* y}{\nu} \quad . \tag{10}$$

In connection with the turbulent velocity distribution represented by Eq. (7), the values of the constants using k = 0.4 and s = 11.6 are

$$A = 5.75 \quad \text{and} \quad B = 5.50 \quad . \tag{11}$$

Schlichting [Ref. (1)] suggests a slight empirical modification of these values for flat plates to

$$A = 5.85 \quad \text{and} \quad B = 5.56 \quad , \tag{12}$$

so that Eq. (6) finally takes the form

$$\varphi = 5.85 \log \eta + 5.56 \quad . \tag{13}$$

This result, along with Eq. (10) for the sublayer velocity distribution, is usually referred to as the "law of the wall." A plot of φ as a function of η is presented in Fig. 1 in semilogarithmic form, based on Eqs. (10) and (13).

When compared with experimental evidence, two deviations from the analysis on which Fig. 1 is based are immediately evident. The transition from the laminar sublayer to the main turbulent flow is not instantaneous as assumed in the theory at $\eta = 11.6$, but rather takes place over a finite portion of the complete boundary layer. The other difference is found in the outer portion of the boundary layer where the values of φ tend to be somewhat larger than those predicted by the analysis. A good comparison with experimental data for incompressible flow in smooth pipes is found in Fig. 20.4 of Ref. (1). Similar plots can also be drawn for flat plate boundary layers, although in this case a complete analysis requires a determination of local shear stress τ_o in order to evaluate the factor u*. Such comparisons will be given later in connection with compressible flows.

2.2 Determination of Skin Friction Coefficients

The results contained in the "law of the wall" equation may be used as a basis for calculating the values of both local and mean skin friction coefficients. The local value at a point on the plate at a distance x from the leading edge is given by the relation

$$c_f = 2\tau_o/\rho u_1^2 \quad , \tag{14}$$

while the Reynolds Number based on the same distance is

$$R = \rho u_1 x/\mu \quad , \tag{15}$$

the assumption here being that the boundary layer is completely turbulent beginning at the leading edge. If these values are used to determine the shear stress and the friction-distance parameter, it is found that the skin friction coefficient and the Reynolds Number are related by the expression

$$1/\sqrt{c_f} = 1.7 + 4.15 \log (c_f R) \quad . \tag{16}$$

The numerical coefficients in Eq. (16) are based on the values of A and B represented by Eq. (13).

If the value of the mean skin friction coefficient is desired, representing the drag force on one side of the plate, it may be written in the form

$$C_F = 2D_f/\rho u_1^2 x \quad . \tag{17}$$

The determination of the value of the drag force D_f is made by using the Von Kármán-Pohlhausen momentum integral formula. For one side of the flat plate in incompressible flow, this relation is simply

$$D_f = \rho \int_0^\delta u(u_1-u)dy \quad . \tag{18}$$

Introduction of the law of the wall velocity distribution for u, carrying out the integration across the boundary layer at a particular value of x, and the omission of negligible terms in the result finally lead to the so-called Von Kármán-Schoenherr formula, which is

$$0.242/\sqrt{C_F} = \log(C_F R) \quad . \tag{19}$$

Equation (19) has the disadvantage that it is not possible to solve it explicitly for C_F as a function of R, although the converse relation is readily obtainable. Schlichting [Ref. (1), p. 602] has therefore proposed an alternate relation which closely approximates Eq. (19) over a wide range of Reynolds Numbers and is of the form

$$C_F = 0.455/(\log R)^{2.58} \quad . \tag{20}$$

If the boundary layer has an initial segment of laminar flow, followed by a transition to turbulent flow, an analysis by Prandtl and Schlichting [Ref. (1), p. 602] leads to a relation of the form

$$C_F = 0.455/(\log R)^{2.58} - K/R \quad . \tag{21}$$

This result is based on the combination of the Blasius formula for a laminar incompressible boundary layer,

$$C_F = 1.328/(R)^{1/2} \quad , \tag{22}$$

with the turbulent skin friction relation of Eq. (20). The value of the coefficient K in Eq. (21) depends upon the Reynolds Number at which the transition to turbulent flow begins. This in turn depends on the shape of the plate leading edge, the level of free stream turbulence in the case of a wind tunnel test, and the roughness of the plate surface, particularly in the vicinity of the leading edge. A typical value of this critical Reynolds Number is 5×10^5, which leads to a value of K = 1700. The results represented by Eqs. (20), (21), and (22) are shown in Fig. 2 in a typical logarithmic plot.

2.3 The Velocity Defect Law

As already mentioned, the law of the wall relation of Eq. (6) does not agree too well with experimentally determined velocity distribution data for large values of η. This is due primarily to the fact that the law of the wall was derived on the basis of conditions in the immediate vicinity of the wall or boundary surface.

If instead the integration of the basic relation of Eq. (1) is carried out using conditions at the outer edge of the boundary layer, i.e.,

$$y = \delta \, , \; u = u_1 \quad \text{and} \quad \partial u/\partial y = 0 \quad , \tag{23}$$

a relation of the form

$$\varphi_1 - \varphi = -A \log(y/\delta) - C \tag{24}$$

is obtained. The value of the constant A is found to be 5.75, as in the case of the law of the wall, and this value holds for both pipe and boundary layer flows. The value of the second constant, C, may vary widely depending on the nature of the boundary conditions. For smooth pipe and channel flow, a value of C = -0.85 appears to be satisfactory, while for boundary layer flows, C = -3.25. The relationship of Eq. (24) is frequently referred to as the "velocity defect law," since the difference $\varphi_1 - \varphi$ is essentially the difference between the velocity outside the boundary layer and the value within it for values of y approaching the boundary layer thickness δ. Both values are of course expressed as ratios to the friction velocity, u*.

In comparing the law of the wall and the velocity defect law, it should be noted that the former expresses φ as a function of the friction-distance parameter $\eta = yu^*/\nu$, while the latter gives φ as a function of y/δ. Thus, if both laws are to be shown graphically on the same plot, it is necessary to change from one independent variable to the other. This change may be accomplished by writing

$$\frac{y}{\delta} = \frac{yu^*}{\nu} \frac{\nu}{u^*\delta} = \eta\left(\frac{\nu}{u^*\delta}\right) \quad .$$

The friction velocity is then written out as $u^* = \sqrt{\tau_o/\rho}$ and the shear stress is expressed in terms of the local skin friction coefficient, c_f, with the result that

$$\frac{y}{\delta} = \eta\left(\frac{\nu}{u_1\delta}\right)\sqrt{\frac{2}{c_f}} \quad . \tag{25}$$

Thus, it is necessary to have information available as to the value of the boundary layer thickness δ, or its Reynolds Number $R_\delta = \frac{u_1\delta}{\nu}$, and also the value of c_f in order to accomplish the desired transfer. In Ref. (2), Schultz-Grunow used extensive data from measurements of the turbulent boundary layer on a flat plate to develop this idea further, including expressions for R_δ and for c_f. He then plotted his velocity profile data both as a function of η, as well as a function of y/δ. His plot in the latter form is shown in Fig. 3 and clearly illustrates the significance of the velocity defect law as it applies to the outer portion of the boundary layer.

2.4 The Law of the Wake

An extension of the velocity defect concept has been developed by Coles [Ref. (3)], a brief summary of which is given in an article by W. C. Reynolds [Ref. (4)]. The results of Coles' analysis as summarized in Reynolds' article are given in the so-called "law of the wake" which may be written in the form

$$\varphi_1 - \varphi = -\frac{1}{k}\,\ell n(y/\delta) + \frac{\Pi}{k}\,[2-w(y/\delta)] \quad . \tag{26}$$

The coefficient Π is described as a "wake factor" which is related to the shape parameter H_{12} and the local skin friction coefficient c_f.

The shape parameter used here is the usual value determined by the ratio of the displacement and momentum thicknesses, that is,

$$H_{12} = \delta_1/\delta_2 \quad . \tag{27}$$

The value of k is the usual Prandtl-Nikuradse mixing length factor, taken as 0.4 in the present discussion. Finally the function $w(y/\delta)$ is Coles' wake function which he originally gave in numerical form and which has been approximated by various empirical relations. Typical of the latter are the transcendental relation

$$w(y/\delta) = 1 - \cos(\pi\eta) \tag{28}$$

used by Hinze and Spalding and the polynomial form suggested by Rotta [Ref. (5)],

$$w(y/\delta) = 39\eta^3 - 125\eta^4 + 183\eta^5 - 133\eta^6 + 38\eta^7 \quad . \tag{29}$$

Rotta indicates that the law of the wake may be used to obtain a relation for the local skin friction coefficient in the form

$$\sqrt{2/c_f} = \frac{1}{k} \ln\left(\frac{u_1 \delta_1}{\nu}\right) + C' + K' \quad , \tag{30}$$

where δ_1 is the displacement thickness of the boundary layer. He indicates that C' is the usual constant value of 5.2 appearing in the law of the wall relation, while the value of the second constant is indicated to be obtainable as a function of the wake factor Π.

The numerical values of Coles' laws were given in Ref. (3) for the wall region as well as for the outer portion of the boundary layer. These values were based on an extensive analysis of all

experimental data then available and resulted in the values given here in Table I. The basic relations to which these data apply are the law of the wall, written in the form

$$\varphi = f_1(\eta) \quad , \tag{31}$$

and the velocity defect law,

$$\varphi_1 - \varphi = f_2\left(\frac{y}{\delta}\right) \quad . \tag{32}$$

It is now quite generally accepted practice to use these values, or empirical relations based on them, in lieu of expressions such as Eqs. (13) and (24) which were derived from mixing length theory.

In connection with these last two references, it should be noted that the paper by Reynolds appears in the Proceedings of an invited conference held at Stanford University in the summer of 1968, in which an international group of workers in the turbulent boundary layer field who had developed various calculation methods presented their procedures as applied to a number of selected incompressible flow problems. These methods were subjected to a close critical evaluation of their effectiveness, so that this publication represents a comprehensive summary of the state-of-the-art at the time of its publication. The Proceedings also includes a paper by Rotta which presumably covers some of his later work in this field beyond that represented by Ref. (5). The methods considered by the Stanford conference were limited to incompressible flows, but included some considerations of roughness and external pressure gradient effects.

III. TURBULENT BOUNDARY LAYERS IN COMPRESSIBLE FLOW

The development of interest in the boundary layer problems of compressible fluids is actually one of long standing, as evidenced by the application to such flows in high-speed fluid machinery involving gaseous fluids and in aeroballistics. Active research in this area did not progress substantially until the development of high-speed aircraft and guided missiles; in fact, it was in connection with design problems in the latter field that the ARL boundary layer research program was initiated late in 1947. A dual approach was formulated, involving an extension of incompressible flow boundary layer theory, as well as an experimental program of velocity distribution measurements and skin friction determinations. The next sections of this report will present a summary of some of the more significant work concerned with the analytical phase of the program.

3.1 Boundary Layer Theory for Compressible Fluids

An early approximate method of estimating skin friction in a compressible fluid was devised by Von Kármán [Ref. (6)], based on the concept of replacing the free stream values of viscosity and density by values corresponding to the wall temperature. The temperature itself is determined by writing the energy equation without dissipation for a local point in the flow and the free stream, that is,

$$C_p T + \frac{u^2}{2} = C_p T_1 + \frac{u_1^2}{2} = C_p T_w \quad . \tag{33}$$

The introduction of the free stream Mach Number M_1 makes it possible to solve for the ratio of local and wall temperatures, the result being

$$\frac{T}{T_w} = 1 - \left(\frac{\gamma-1}{2}\right) M_1^2 \left(\frac{T_1}{T_w}\right)\left(\frac{u}{u_1}\right)^2 \quad . \tag{34}$$

When applied to free stream conditions, $u = u_1$ and $T = T_1$, Eq. (34) becomes

$$\frac{T_w}{T_1} = 1 + \frac{(\gamma-1)}{2} M_1^2 \quad . \tag{35}$$

The introduction of this value in Eq. (34) finally gives for the ratio of local and wall temperatures the expression

$$\frac{T}{T_w} = 1 - \sigma\left(\frac{u}{u_1}\right)^2 \quad , \tag{36}$$

where

$$\sigma = \frac{m}{1 + m} \tag{37}$$

and

$$m = \frac{(\gamma-1)}{2} M_1^2 \quad . \tag{38}$$

All of this analysis is based on the assumption that there is no significant heat transfer at the wall and no dissipation of energy within the boundary layer.

The density is next assumed to be inversely proportional to the temperature, while the viscosity relation may be approximated by a simple exponential relation of the form

$$\frac{\mu}{\mu_1} = \left(\frac{T}{T_1}\right)^{\omega} \quad , \tag{39}$$

with $\omega = 0.768$ for air. The introduction of the wall values in the simple boundary layer momentum theory, based on a one-seventh power velocity distribution, yields the result that

$$\frac{C_F}{C_{F_i}} = \left(\frac{T_w}{T_1}\right)\frac{\omega - 4}{5} \quad . \tag{40}$$

The same procedure can also be carried out on the basis of the law of the wall skin friction formula, Eqs. (6) and (19), with the result that

$$\frac{0.242}{\sqrt{C_F}} = \left(\frac{T_w}{T_1}\right)^{1/2}\left[\log(C_F R_1) - \omega \log\left(\frac{T_w}{T_1}\right)\right] \quad , \tag{41}$$

where T_w/T_1 is calculated from Eq. (35). Either Eq. (40) or (41) may be used to calculate the ratio of the compressible and incompressible values of the skin friction coefficients as functions of free stream Mach Number, the results being shown in Fig. 4.

A more rigorous analysis of the compressible turbulent boundary layer was carried out by Wilson [Ref. (7)] as the initial analytical part of the ARL program. He developed his analysis by beginning with the Prandtl mixing length relation of Eq. (1) and the Von Kármán mixing length formulation of Eq. (3), with the density and viscosity

terms being expressed in terms of the wall temperature as in the preceding case, but with the modification of introducing a temperature recovery factor,

$$r = \frac{T_w - T_1}{T_{w_{ad}} - T_1} \quad , \tag{42}$$

so that

$$\frac{T_w}{T_1} = 1 + r\left(\frac{\gamma-1}{2}\right) M_1^2 \tag{43}$$

replaces the relation of Eq. (35). The integration, which is rather lengthy, finally leads to a law of the wall for a compressible boundary layer in the form

$$\eta \cong \frac{k\varphi_1 s}{k^2\varphi_1^2+\sigma}\left[k\varphi_1\sqrt{1 - \sigma\left(\frac{\varphi}{\varphi_1}\right)^2} + \sigma\left(\frac{\varphi}{\varphi_1}\right)\right]e^{\beta} \quad , \tag{44}$$

$$\beta = \frac{k\varphi_1}{\sigma^{1/2}}\left[\sin^{-1}\left(\frac{\sigma^{1/2}\varphi}{\varphi_1}\right) - \sin^{-1}\left(\frac{\sigma^{1/2}s}{\varphi_1}\right)\right] \quad . \tag{45}$$

The values of φ and φ_1 are the velocity ratios, u/u*, within and at the outer edge of the boundary layer, as in the incompressible case, while s again is the value corresponding to the outer edge of the laminar sublayer. When converted to logarithmic form, Eq. (44) becomes

$$\left(\frac{\varphi_1}{\sqrt{\sigma}}\right)\sin^{-1}\left(\frac{\varphi\sqrt{\sigma}}{\varphi_1}\right) = \frac{1}{K}\left(\ell n\eta + \ell n\left(\frac{e^{ks}}{s}\right)\right) = f(\eta) \quad , \tag{46}$$

but instead of evaluating the right-hand side of this expression in terms of η, present practice is to assume that the right side may be regarded as a function of η which is best defined by the numerical data established by Coles [Ref. (3)], which have been used as a basis for plotting the curve shown in Fig. 4. It is significant to note that when plotted in this form, the curve of Fig. 4 is independent of Mach Number. Also the transition from the laminar sublayer to the main turbulent portion of the boundary layer is included in Coles' data. Included in Fig. 4 are some experimental measurements made at ARL for several Mach Numbers and for slight variations in the momentum thickness Reynolds Numbers, R_{δ_2}. These data are taken from the work of Fenter and Stalmach [Ref. (8)] and show the trend away from the law of the wall into the law of the wake for the larger values of η.

Wilson did not undertake a comparison with either the law of the wall or the law of the wake using his velocity profile measurements. He did, however, transform the results represented by Eq. (46) into a relation between mean skin friction coefficient and Reynolds Number. This was accomplished by first introducing values of C_{F_*} and R_*, both based on density and viscosity values at the plate surface. A further transformation, introducing free stream values of these latter quantities and integrating along the plate by means of the momentum equation, finally led to the result that

$$0.242\left(\frac{\sin^{-1}\sigma^{1/2}}{\sigma^{1/2}}\right)\sqrt{(1+rm)C_F} = \log\,(C_F R_1) - \omega \log\,(1+rm) \quad . \qquad (47)$$

Attention is invited to the fact that σ and m are the Mach Number functions defined by Eqs. (37) and (38). It should also be noted that Eq. (47) is based on Wilson's original form as given by Eq. (46), rather than on Coles' data for $f(\eta)$.

The result of Eq. (47) closely resembles the Von Kármán-Schoenerr formula of Eq. (19), except for the modifications represented by the presence of the Mach Number functions, σ and m, and the temperature recovery factor r. An important feature of these results may be demonstrated by a rearrangement of Eq. (47) into the form

$$\frac{0.242}{\left[\sigma(1+m)/(\sin^{-1}\sigma^{1/2})^2\right]^{1/2}\sqrt{C_F}} = \log\left\{\left[\frac{\sigma(1+m)}{(\sin^{-1}\sigma^{1/2})^2}\right] C_F\left[\left(\frac{\sin^{-1}\sigma^{1/2}}{\sigma^{1/2}}\right)^2 (1+m)^{(1+\omega)}\right]\right\}R_1 \quad , \tag{48}$$

or by replacing the two Mach Number functions by

$$X = \frac{(1+m)C_F}{(\sin^{-1}\sigma^{1/2})^2} \tag{49}$$

and

$$Y = \frac{(\sin^{-1}\sigma^{1/2})^2}{\sigma}(1+m)^{-(1+\omega)}R_1 \quad . \tag{50}$$

Eq. (48) may be written in the condensed form

$$\frac{0.242}{X^{1/2}} = \log XY \quad . \tag{51}$$

The important feature of this result is that a plot of X as a function of Y is obtained as a single universal curve which is the same for all Mach Numbers. For numerical calculations, it is

necessary to solve for Y as a function of X, or in effect, Reynolds Number as a function of skin friction coefficient. This form is

$$\log Y = \frac{0.242}{X^{1/2}} - \log X \quad . \tag{52}$$

A further simplification in the calculation procedure is obtained by separating out the portions of X and Y which are dependent on Mach Number only. This is accomplished by writing

$$X = C_F X' \tag{53}$$

and

$$Y = R_1 Y' \quad , \tag{54}$$

where

$$X' = \frac{\sigma(1+m)}{\left(\sin^{-1}\sigma^{1/2}\right)^2} \tag{55}$$

and

$$Y = \frac{\left(\sin^{-1}\sigma^{1/2}\right)^2}{\sigma(1+rm)^{1+\omega}} \quad . \tag{56}$$

Graphs showing the variation in the several Mach Number functions are presented in Figs. 5 and 6. In the first of these figures the value of the term $1 + rm$ is shown for two values of the recovery factor, $r = 1.00$ and $r = 0.88$, in order to illustrate the small effect of this factor. In Fig. 6 are shown the values of $1/(1 + m)$ and $(1 + m)^{1+\omega}$ for $\omega = 0.768$, the additional Mach Number factors required.

Figures 7 and 8 show the values of the parameters X' and Y', as well as their reciprocals, all as functions of Mach Number. Making use of all of these factors, it is now possible to compute the data represented by the curve shown in Fig. 9. This is the universal relation between skin friction coefficient and Reynolds Number described by Eqs. (51) or (52). The curve of Fig. 9 was used as a basis for determining the actual values of C_F as a function of Reynolds Number, R_1, for three different values of the free stream Mach Number, that is, $M_1 = 0$ corresponding to imcompressible flow and two supersonic values, $M_1 = 5$ and $M_1 = 10$, plotted in Fig. 10. Finally curves are plotted in Fig. 11 showing the ratio of the compressible and incompressible values of C_F, this being done for an assumed Reynolds Number of 10^7. Similar curves are also shown based on Von Kármán's early analysis which led to Eq. (41), the two values of the recovery factor again being considered. All of these curves are shown as functions of Mach Number in Fig. 11.

In this connection reference should also be made to a more recent work by Wilson [Ref. (8)] which includes some of the previous material on smooth, adiabatic plates but also adds more recent work on heat transfer and roughness effects.

IV. THE EFFECTS OF SURFACE ROUGHNESS

The determination of the effects of roughness on the character of the boundary layer flow is a problem of long standing. One of the earliest systematic investigations was the work of Nikuradse which actually involved pipe flow rather than boundary layer flow. In both cases, however, roughness patterns may be classified as (1) uniformly distributed, (2) distribution of isolated roughness elements, and (3) various special patterns which do not fall into either of the first two categories. Nikuradse's work on pipe flow was accomplished by coating the interior wall with sand grains of a specified average size and then determining the longitudinal pressure drop and the velocity distribution across the pipe. This variety of roughness falls in the category of the uniformly distributed type, although the precise shape of the roughness particles could have varied substantially. In some of the early work done at ARL on the boundary layer roughness problem, uniformly distributed roughness was described as being of the "Rocky Mountain type," exemplified by the distributed sand grains, or of the "Mole Hill type" when the roughness particles are smooth and regular, such as would be the case when small spherical beads constituted the roughness elements.

4.1 Roughness Effects in Incompressible Flow in Pipes

A comprehensive summary of Nikuradse's work with what was essentially incompressible flow is given in Ref. (1), Chaps. XX-f and XXI-c. The mechanism of the flow has been well demonstrated in terms of boundary layer concepts by recognizing the fact that for

a given roughness particle size and considering flows with increasing Reynolds Number, the boundary layer initially completely covers the roughness projections so that the friction factor as a function of Reynolds Number follows closely the variation found for smooth surfaces. As the Reynolds Number increases, there is a steady decrease in boundary layer thickness until a point is reached where the roughness elements extend through it into the main turbulent portion of the flow. There is thus an augmentation of the turbulent flow losses and a gradual leveling off of the friction factor for further increases in Reynolds Number. The conditions at which this situation develops have been referred to as "admissible" or "threshold roughness." There is also a change in the velocity distribution across the pipe, characterized by a relation of the form

$$\frac{u}{u^*} = 5.75 \log\left(\frac{y}{k_s}\right) + B \quad , \tag{57}$$

where

(1) u is again the local mean velocity at a distance y from the pipe wall,

(2) u^* is the friction velocity,

(3) k_s is the average diameter of the sand grain particles, and

(4) B is a factor which is a function of the roughness Reynolds Number, u^*k_s/ν. The nature of the variation in B is described by the plot of Fig. 12.

On the basis of these data, smooth pipe flow may be considered as corresponding to roughness Reynolds Numbers, $u^*k_s/\nu < 5$, in which case B is essentially a linear function of u^*k_s/ν of the form

$$B = 5.56 + 5.85 \log (u^*k_s/\nu) \quad . \tag{58}$$

There next follows a transition zone in which B rises to maximum and then decreases slightly to about 8.5 in the completely rough zone. These three zones are then characterized by the following values of the roughness Reynolds Number:

$$\text{Hydraulically smooth: } (u^*k_s/\nu)<5$$
$$\text{Transition: } 5<(u^*k_s/\nu)<70$$
$$\text{Completely rough: } (u^*k_s/\nu)>70 \quad .$$

Additional studies of rough pipes have shown that in the case of isolated roughness patterns with roughness elements located at discrete points, and for commercial pipe of various types, the roughness can be expressed in terms of an equivalent sand grain roughness; these results are also summarized in Ref. (1).

4.2 Roughness Effects in Incompressible Flow on Flat Plates

Prandtl and Schlichting [Ref. (10)] made a very useful extension of Nikuradse's pipe flow research by applying his results to flat plates as affected by sand grain roughness. They also demonstrated that the concept of admissible roughness continued to be applicable, with the value of the admissible sand grain dimension given by

$$k_{adm} \leqq 100\nu/U_\infty \quad . \tag{59}$$

In addition to an elaborate set of charts for estimating roughness effects on flat plate skin friction, interpolation formulas were suggested for local and mean skin friction coefficients. These relations are

$$c_f = \left[2.87 + 1.58 \log \left(\frac{x}{k_s}\right)\right]^{-2.5} \tag{60}$$

and

$$C_F = \left[1.89 + 1.62 \log \left(\frac{\ell}{k_s}\right)\right]^{-2.5} \quad , \tag{61}$$

in which ℓ is the total length of the plate and x is the distance along the plate from its leading edge to the point where the local skin friction coefficient is to be calculated. These relations are considered valid for $10^2 < \ell/k_s < 10^6$.

4.3 Roughness Effects in Compressible Flow on Flat Plates

In a rather detailed study of the effects of roughness on flat plates, Fenter [Ref. (11)] suggested that the factor B in Eq. (57) could be conveniently approximated by a series of linear semilogarithmic relations. Using the type of roughness function for flat plates, the law of the wall is developed in terms of the mean roughness height k_r, and the corresponding value of the friction-distance parameter is then written as

$$\eta_r = k_r u^*/\nu_w \quad . \tag{62}$$

The law of the wall for a roughened plate may then be shown to take the form

$$\varphi = A_r \log(y/k_r) + B_r \quad . \tag{63}$$

The first coefficient, A_r, is equal to A as in Eq. (6) for smooth surfaces; that is, $A_r = A = 5.75$. Equation (63) may be expanded into the form

$$\varphi = A_r \log y - A_r \log k_r + B_r \tag{64}$$

in which the roughness effect is now represented by the last two terms; that is

$$B_r' = B_r - A_r \log k_r \quad . \tag{65}$$

In order to include the smooth plate case in this analysis, Fenter replaced Eq. (65) by the expression

$$B_r' = B - f(\eta_r) \quad , \tag{66}$$

where B = 5.50 is the value previously used in the incompressible smooth surface case and $f(\eta_r)$ is a new roughness function which, on the basis of the linear approximations referred to previously, may be written in the form

$$f(\eta_r) = a \log \eta_r - b \quad . \tag{67}$$

This modified roughness function was assumed to be determined directly from Nikuradse's incompressible pipe flow data given in Fig. 12. The values of $f(\eta_r)$ for the three flow regimes, along with the corresponding forms of Eq. (67), are plotted as functions of log η_r in Fig. 13. The values of the coefficients a and b and the ranges of values of η_r are given in Table I. It should be noted that the value of η_r denoting the demarcation between the transition and the fully rough regimes has been taken as $\eta_r = 100$, instead of the slightly lower value of 70 suggested by Schlichting. A similar treatment of the roughness function

was also used by Young [Ref. (12)] in a later phase of the ARL program, involving heat transfer as well as roughness but subdividing the roughness zones into as many as five segments, as shown in Fig. 12. It is probable that a single functional relation could be established for $f(\eta_r)$ covering the full range of η_r values, but this has not been undertaken up to the present time.

4.4 Roughness and Heat Transfer Effects in Compressible Flow

Fenter included in his work presented in Ref. (11) an extension of the theoretical analysis leading to integrated forms of the velocity profile results which finally yield relations for the local and mean skin friction coefficients as functions of Reynolds Number. Actually the theory was developed in a rather general form so as to include simultaneously the effects of both roughness and heat transfer. While the basic approach was comparable to that used by Wilson [Ref. (7)] in his earlier treatment of compressible flow on a smooth adiabatic plate, the details are considerably more formidable. After a fairly extensive analysis, Fenter's results indicate that the law of the wall velocity profile may be written as

$$\varphi^* + \frac{1}{k} \ell n\, \beta = \frac{1}{k} \ell n \left(\frac{y}{k_r}\right) + C \qquad (68)$$

for a fully rough surface. The factors φ^*, β, and C appearing in Eq. (68) are defined as

$$\varphi^* = \frac{\varphi_1}{\sqrt{\sigma}} \left[\sin^{-1} \left(\frac{2\sigma\varphi/\varphi_1 - \lambda}{\sqrt{\lambda^2+4\sigma}} \right) + \sin^{-1} \left(\frac{\lambda}{\sqrt{\lambda^2+4\sigma}} \right) \right] , \qquad (69)$$

$$\beta = \frac{(k\varphi_1)^2 \sqrt{\lambda^2+4\sigma}}{2\sqrt{\sigma}\left[(k\varphi_1)^2+\sigma\right]} \left[\sqrt{1 - \frac{(2\sigma\varphi/\varphi_1-\lambda)^2}{\sqrt{\lambda^2+4\sigma}}} + \frac{\sqrt{\sigma}\,(2\sigma\varphi/\varphi_1-\lambda)}{k\varphi_1\sqrt{\lambda^2+4\sigma}} \right] , \qquad (70)$$

$$C = 8.5 \quad . \qquad (71)$$

The value of σ is the Mach Number function previously introduced in Eq. (36); that is,

$$\sigma = \frac{m}{1+m} = \frac{\frac{\gamma-1}{2} M_1^2}{1 + \frac{\gamma-1}{2} M_1^2} \quad , \qquad (72)$$

while

$$\lambda = \frac{1+m}{T_w/T_1} - 1 = \frac{1 + \frac{\gamma-1}{2} M_1^2}{T_w/T_1} - 1 \quad . \qquad (73)$$

The corresponding form of the velocity defect law is

$$\varphi_1^* - \varphi^* = F(y/\delta) \quad , \qquad (74)$$

where $F(y/\delta)$ is based on the Coles' function given in numerical form in Table II.

A similar approach to the boundary layer problem for rough surfaces with heat transfer was developed by Van Driest [Ref. (13)] using Prandtl's mixing length theory with Von Kármán's relation for the mixing length term itself. These results were utilized by Young [Ref. (12)] to provide a basis of comparison between theory and experiment in connection with an experimental study of Veegroove type roughness coupled with heat transfer on a flat plate. Van Driest's method of calculation was also included in an extensive comparison of

theories with experimental data by Spalding and Chi [Ref. (14)], the conclusion being that Van Driest's approach appeared to be the most satisfactory. The only important restriction in the development of Van Driest's method was that the Prandtl Number was assumed to be constant and equal to unity.

By making use of the momentum integral relation, both Fenter's and Van Driest's results may be used to derive an expression for the local skin friction coefficient in terms of the momentum thickness Reynolds Number. In the form given by Fenter, this result is

$$\frac{\psi}{\sqrt{\sigma}} \sqrt{\frac{T_1}{T_w}} \frac{1}{\sqrt{c_f}} = 4.13 \log R_{\delta_2} - \frac{f}{\sqrt{2}} + 4.13\omega \log \frac{T_1}{T_w} + 2.90 \quad . \qquad (75)$$

The skin friction coefficient in Eq. (75) is based entirely on free stream conditions, that is

$$c_f = \frac{\tau_o}{\rho_1 u_1^2/2} \quad . \qquad (76)$$

Similarly, the momentum thickness Reynolds Number is

$$R_{\delta_2} = \frac{\rho_1 u_1 \delta_2}{\mu_1} \quad . \qquad (77)$$

The other factors in Eq. (75) are

$$\psi = \sin^{-1}\left(\frac{2\sigma-\lambda}{\sqrt{\lambda^2+4\sigma}}\right) + \sin^{-1}\left(\frac{\lambda}{\sqrt{\lambda^2+4\sigma}}\right) \quad ,$$

which on comparison with Eq. (69) for φ^* will be seen to be equivalent to $\varphi^* \sqrt{\sigma}/\varphi_1$ when $\varphi = \varphi_1$. The factor f in Eq. (75) is the roughness function $f(\eta_r)$ previously discussed and represented by the plot of Fig. 13. Finally it should be noted that the value of η_r may be determined from the relation

$$\eta_r = \frac{k_r u^*}{\nu} = \left(\frac{T_1}{T_w}\right)^{\omega+1/2} R_r \sqrt{\frac{c_f}{2}} \quad , \tag{78}$$

R_r being the Reynolds Number based on the mean height of the roughness elements and the free stream velocity and viscosity. The numerical factors in Eq. (75) have been modified slightly from those calculated from the law of the wall, to obtain somewhat improved agreement with experimental results.

For engineering purposes, it is convenient to have available plots of mean skin friction coefficients as functions of the normal Reynolds Number based on distance along the plate surface. Such plots were first prepared by Moody [Ref. (15)] for roughened pipes, with the roughness Reynolds Number based on the equivalent sand grain roughness dimension as a parameter. Similar plots for roughened flat plates are given by Prandtl and Schlichting [Ref. (10)] based on the assumption that the flow is turbulent from the leading edge rearward. An additional presentation of flat plate data for a range of Mach Numbers up to 5.0 has been developed by Clutter [Ref. (16)] and is also presented by Wilson [Ref. (9)]. Clutter's calculations are based on Van Driest's analysis for the smooth plate and on a simplified treatment of the roughness problem developed by Liepmann and Goddard [Ref. (17)].

The inclusion of heat transfer effects on boundary layer flows has already been discussed to some extent in connection with the preceding analysis. Only the simplest case of a variation in plate

or wall temperature as compared to the adiabatic or zero heat transfer case will be considered. In general the case of heat transfer to or from the plate may be described in terms of the ratio of wall temperature to free stream temperature, this being represented by the factor T_w/T_1 which appears in the equations just presented. No attempt will be made here to discuss the more complicated case of an ablating surface which may introduce a film of molten plate material along with the possibility of chemical reactions taking place in this region.

In addition to the determination of local and mean skin friction coefficients along with boundary layer velocity profiles, it is usually important to provide a means for the calculation of heat transfer rates. This evaluation may be accomplished in terms of a variety of parameters in addition to the flow factors of Reynolds Number and Mach Number. The latter terms are primarily related to similarity conditions based on the momentum or Navier-Stokes equations, while the heat transfer parameters are obtained by similar analyses of the energy equation. The first of these parameters, the so-called Prandtl Number, is defined as

$$P = \mu c_p/\lambda \quad . \tag{79}$$

It is interesting to note that the Prandtl Number is dependent only on the physical properties of the fluid and not on any of the flow characteristics. It may be interpreted physically as a representation of the ratio of the rate of diffusion of vorticity, μ/ρ, to the rate of diffusion of heat, $\lambda/\rho c_p$, where λ is the thermal conductivity and c_p is the specific heat at constant pressure. The thermal conductivity factor is first encountered in writing down the basic Fourier relation for convective heat transfer, that is,

$$q = \lambda\left(\frac{\partial T}{\partial y}\right)_{y=0} \quad , \tag{80}$$

where q is the heat transfer rate per unit time and unit area of the surface.

Another factor of importance in determining heat transfer is the combination of temperatures known as the Eckert Number, defined as

$$E = \frac{2(T_s - T_1)}{T_w - T_1} \quad , \tag{81}$$

where the new term, T_s, is the temperature at a stagnation point. Assuming fully adiabatic conditions, the value of T_s is determined by the adiabatic temperature rise,

$$T_s - T_1 = (\Delta T)_{ad} = u_1^2/2c_{p_1} \quad . \tag{82}$$

Equations (81) and (82) may be combined to yield a relation between the Eckert and Mach Numbers of the form

$$E = \frac{2m\, M_1^2}{(T_w/T_1)-1} \quad . \tag{83}$$

The heat transfer rate determined by Eq. (80) may also be expressed in terms of a heat transfer coefficient and the difference between the recovery temperature and the actual wall temperature. Thus

$$q = h(T_r - T_w) \quad , \tag{84}$$

where T_r corresponds to the condition that $\left(\frac{\partial T}{\partial y}\right)_{y=0} = 0$. The combination of Eqs. (80) and (84) gives

$$\lambda\left(\frac{\partial T}{\partial y}\right)_{y=0} = h(T_r - T_w) \quad , \tag{85}$$

which may be nondimensionalized by writing $y = y'\ell$, with ℓ as a geometric scale factor, and $T = T'(T_r - T_w)$ for the local temperature. Equation (85) then reduces to the form

$$\left(\frac{\partial T'}{\partial y'}\right)_{y'=0} = \frac{h\ell}{\lambda} \quad , \tag{86}$$

which defines a new nondimensional heat transfer parameter known as the Nusselt Number. Still another parameter may be introduced by arbitrarily inserting the Prandtl Number and the Reynolds Number in Eq. (86). This procedure shows that the Nusselt Number may then be expressed as

$$N = PR\left(\frac{h}{\rho\, c_p\, u_1}\right) \quad , \tag{87}$$

where the new combination

$$\frac{h}{\rho\, c_p\, u_1} = S \tag{88}$$

is known as the Stanton Number.

There are additional heat transfer parameters known as the Peclet Number and the Grashof Number, but these are not pertinent to the present discussion. A comprehensive summary of these elements of heat transfer theory can be found in Ref. (1), Chap. XII, based on laminar boundary layer theory. In the case of turbulent boundary layers, the same factors are utilized, its being necessary to make use of equivalent or eddy viscosity and conductivity.

Approximate solutions to an important group of gas flow problems may be obtained by assuming that the Prandtl Number is equal to unity. This assumption leads to considerable simplification of the basic equations and, in the case of air, is not too far from reality. For air over a moderate range of temperatures, the Prandtl Number has a value between 0.71 and 0.72. If the Prandtl Number is assumed to be unity, it may be shown that the temperature within a boundary layer is given by the Crocco relation as a function of local velocity; that is,

$$T/T_1 = T_w/T_1 - (T_w/T_1 - 1)\, u/u_1 + m(u/u_1)(1 - u/u_1) \quad . \tag{89}$$

For the more general case where the Prandtl Number is a variable and not equal to unity, Harkness [Ref. (18)] has suggested the replacement of the quadratic relation of Eq. (89) by a cubic of the form

$$\begin{aligned} T/T_1 = {} & T_w/T_1 + (c+1)\left[(T_r/T_1) - (T_w/T_1)\right] u/u_1 \\ & + \left[3.627(1 - T_r/T_1) + 2.62\right] m - c\left[(T_r/T_1) - (T_w/T_1)\right](u/u_1)^2 \\ & - 2.627\left[1 + m - (T_r/T_1)\right](u/u_1)^3 \quad . \end{aligned} \tag{90}$$

The coefficient c in this expression is a function of the Prandtl Number of the form

$$c = \frac{m\left[P_w - P_{w_{ins}}\right]}{\left[(T_r/T_1) - (T_w/T_1)\right]} \quad , \tag{91}$$

where P_w and $P_{w_{ins}}$ are respectively the Prandtl Numbers for the actual wall and for insulated wall conditions. In attempting to arrive at a skin friction evaluation, Harkness introduced the assumption that the laminar sublayer thickness was a function of the heat transfer rate. Based on a limited amount of experimental data, this relation is

$$s = s_o + 6.6t \quad , \tag{92}$$

where s is the sublayer parameter $\delta_s u^*/\nu$, $s_o \cong 11.6$ is its value for the zero heat transfer case, and t is a temperature factor of the form

$$t = 1 - T_w/T_r \quad . \tag{93}$$

The integration of the mixing length equation using Harkness's modifications leads to an extremely complicated and awkward form. An alternate approach using a simpler quadratic temperature variation was developed by Moore [Ref. (19)] as a later phase of the ARL program. The relation between temperature and velocity was taken in the form

$$\frac{T}{T_1} = 1 - t'\left(\frac{\varphi}{\varphi_1}\right)^2 = 1 - t'\left(\frac{u}{u_1}\right)^2 \quad , \tag{94}$$

with

$$t' = 1 - \frac{T_1}{T_w} \quad . \tag{95}$$

In addition Moore also used Harkness's relation for the sublayer thickness as given by Eq. (93), with the result that the law of the wall relation becomes

$$\left(\frac{\varphi_1}{\sqrt{\sigma}}\right) \sin^{-1}\left(\frac{\varphi\sqrt{\sigma}}{\varphi_1}\right) - 6.6t + \left(\frac{1}{k}\right) \ell n\left(\frac{s}{s_o}\right) = f(\eta) \quad . \qquad (96)$$

The right side of this expression, $f(\eta)$, is again the Coles' function.

The most straightforward procedure for determining the heat transfer coefficient h is to first calculate the local skin friction coefficient and then to make use of the Reynolds Analogy in a generalized form. The latter connects the Stanton Number with the Reynolds Number by means of the expression

$$S = \frac{h}{\rho\, c_p\, u_1} = \frac{1}{p}\frac{C_f}{2} \quad . \qquad (97)$$

The quantity p is known as the Reynolds Analogy factor and reflects the difference between the actual value of S and that determined by Reynolds' very simple analysis in which he demonstrated that $p = 1$. In general p is primarily a function of Prandtl Number as indicated by the example of Colburn's analysis of heat transfer for low speed turbulent boundary layers for which he found that

$$p = (P)^{2/3} \quad . \qquad (98)$$

This of course gives Reynolds' result when $P = 1$. It would be reasonable to expect that in the case of a high speed flow, the Reynolds Analogy factor would depend on the Mach Number and on some characteristic temperature ratio. In Harkness's analysis he showed that

$$p = \frac{P_w}{1 + c} \quad , \tag{99}$$

where c is the coefficient defined by Eq. (91).

V. EXPERIMENTAL METHODS FOR DETERMINING BOUNDARY LAYER CHARACTERISTICS

A variety of techniques have been developed for the experimental determination of boundary layer characteristics, the nature of which usually depends on the type of information that is desired. Probably the earliest of these methods as applied to flat plates was represented by the work of Kempf [Ref. (20)] who suspended a complete plate from the carriage of a towing tank and measured the total drag force with the plate parallel to the direction of motion. By varying the length of the plate and the towing speed, a range of Reynolds Numbers could be obtained. When applied to measurements made in air, this method was not very satisfactory because of the reduced magnitude of the forces to be determined.

5.1 The Momentum Deficit Method

This procedure is directly related to the momentum integral theory which connects the frictional drag on a portion of the plate surface with the loss of momentum within the boundary layer up to the point where the measurements are made. Since

$$D_f = \int_0^{\delta} \rho u(u_1 - u)\, dy \quad , \tag{100}$$

it is only necessary to determine the local velocity u as a function of y and to compare the integrated value of $\rho u^2 dy$ with that corresponding to the free stream velocity. In the case of a compressible fluid it is of course necessary to calculate the density of the fluid at each point. Values of the velocity are readily determined by means

of a Pitot tube attached to a traversing mechanism so as to give u as a function of y. In the incompressible case the simple Bernoulli Equation provides a relation between Pitot pressure and velocity, while in the compressible case, variations in density must be taken into account, including the use of the Rayleigh-Pitot formula for supersonic flow.

In order to minimize errors due to the dimensions of the Pitot tube, the usual practice is to maintain the transverse dimension, or diameter if the tube is circular, as small as possible consistent with the avoidance of excessive time lags in the transmission of changing pressures to the recording instrument. Such considerations are also important in seeking to obtain velocity measurements close to the plate surface and if possible within the laminar sublayer. For these reasons some experimenters have utilized Pitot tubes with a flattened cross section, the minimum dimension obviously being in the direction normal to the boundary surface. In all cases care must be exercised to insure that the Pitot tube is properly aligned with the main flow direction. Since the measurements are being made in a region with a velocity gradient, there may be some effect on the true pressure reading, or alternately there can be a shift in the position of the effective center of the Pitot tube opening. For tubes of reasonably small diameter, however, this correction is usually negligibly small.

In the case of a laminar boundary layer or within the laminar sublayer of a turbulent one, it may be desirable to obtain readings at a sufficient number of points near the surface so as to determine the velocity gradient with reasonable accuracy. The shear stress at the wall being given by the relation

$$\tau = \mu\left(\frac{\partial u}{\partial y}\right)_{y=0} , \qquad (101)$$

it is apparent that this goal may be difficult to attain, since du/dy must be determined as the slope of an experimentally obtained curve of $u = f(y)$. This problem is avoided in the case of pipe flow by relating the wall shear stress to the longitudinal pressure drop, the latter being a quantity which can be measured with reasonably good accuracy by means of static pressure taps at two stations along the length of the pipe.

5.2 Local Shear Stress Measurements

In view of the fact that the theoretical calculations of turbulent boundary layer characteristics directly involve the wall shear stress, it is apparent that a method for determining the value of this stress has significant advantages. The integrated values such as mean skin friction coefficient can then be calculated with good accuracy. Such considerations have led to the use of floating element balances in which a portion of the boundary surface is separated from the surrounding area and supported by means of a mechanism through which the shear force on the isolated element can be measured. Two principal types of shear stress balances have been developed, the initial work being that of Liepmann and Dhawan [Ref. (21)] who used a null-reading arrangement. Since some clearance around the shear element is required, this system has the advantage that the element is always in the same position when the reading is taken. The other type, used extensively in the ARL program [Ref. (22)], is of the displacement variety, in that the shear element is allowed to move a small distance in the flow direction. This element is supported by cantilever springs to which is attached the core of a linear variable transformer. Displacement of the core causes a change in the output voltage and the relation between this quantity and the applied shear force can be readily determined by calibration. The displacement type of balance is particularly suitable for use in blow-down wind tunnels where short running times

are involved. With both types of balances, it is essential that the shear element be carefully aligned with the surrounding surface. A displacement in either direction normal to the main surface can introduce large errors, while an angular misalignment can likewise be extremely troublesome. Considerable time under the ARL program has been devoted to a study of these alignment problems, with the results being covered primarily in a report by O'Donnell [Ref. (23)] and in a technical journal paper by Westkaemper and O'Donnell [Ref. (24)]. While not directly connected with the Navy supported program at ARL, a fairly extensive study was undertaken for the NASA Langley Research Center leading to the design and construction of improved balances to be operated in supersonic flows with moderately high rates of heat transfer.

In general the design of a satisfactory skin friction balance requires consideration of the range of forces to be measured, these in turn being dependent primarily on the Reynolds Number and the Mach Number. Hence, each balance must be treated as a custom built item adapted to the particular flow environment with which the experiments are concerned. It is always desirable to have as high a degree of sensitivity in the balance as possible, this sensitivity being controlled by the size of the shear disk, the dimensions of the supporting flexures, and the response of the transformer. Since it is desired to obtain shear force readings effectively at the center of the balance disk, a reduction in its size is always desirable. This reduction is limited, however, by the fact that the forces to be measured become decreasingly small, while at the same time the flexure dimensions become so small as to introduce severe stability and vibration problems. The experience at ARL has shown that the minimum disk diameter should not be less than 0.5 in. and preferably of the order of 1.0 in.

5.3 The Preston Tube

A modification of the Pitot tube application was developed in the early years of aerodynamic research by Sir Thomas Stanton at the British National Physical Laboratory. Stanton's idea was to construct a total pressure probe in such a way that the boundary surface itself formed the inner wall of the tube. The overall dimensions could then be made quite small so that the tube was capable of exploring very thin boundary layers including the laminar sublayer. An extension of this scheme was introduced more recently by Dr. J. H. Preston, now at the University of Liverpool [Ref. (25)]. In his application an ordinary Pitot tube of round cross section is moved toward the boundary surface until it is actually in contact with the latter. If the outside diameter of the nose of the tube is d, then the center is at a distance d/2 from the surface. Assuming that the boundary layer is turbulent and that the law of the wall is applicable, Preston then reasoned that there should be a correlation between the surface shear stress at the nose of the tube and the pressure reading recorded by it. As a part of the work reported on in Ref. (11), Fenter made an analysis of the Preston tube in a compressible boundary layer flow, extending a study made by Hsu [Ref. (26)] for the incompressible case, which includes the effects of tube diameter and wall thickness. The significant result of these analyses is that the tube should extend well into the region in which the law of the wall is valid but not into the law of the wake region. Fenter's work demonstrates that the critical or maximum diameter of the tube is given approximately as

$$d_{cr} \cong \frac{0.226x}{t+1} R_x^{-y_5} \quad . \tag{102}$$

Here x is the distance from the plate leading edge to the measuring station, R_x is the corresponding Reynolds Number, and t is the wall

thickness of the nose of the tube. As was the case with the floating element balance, the ARL investigations of the performance of the Preston tube also included the effects of pressure gradients and heat transfer [Refs. (27) and (28)].

VI. RESULTS OF SKIN FRICTION AND HEAT TRANSFER MEASUREMENTS

In general the experimental phase of the ARL program followed in parallel with the analytical work, with the former covering first the use of the momentum deficit method on smooth flat plates under adiabatic conditions. These investigations were next extended to measurements on plates with uniformly distributed roughness, with both the floating element balance and the Preston tube being introduced into the program at this time. The consideration of more regular types of roughness, particularly that consisting of transverse Veegrooves, was studied next with the effects of heat transfer also included, with the smooth, adiabatic plate being included as a limiting case of zero heat transfer and zero roughness. The results of each of these various phases of the experimental program are summarized in the sections which follow.

6.1 Skin Friction Measurements on the Smooth Flat Plate

The measurements on smooth, adiabatic plates were actually an integral part of the program reported on by Wilson in Ref. (7) and involved the application of the momentum deficit method using a traversing Pitot tube across the boundary layer at several stations along the plate center line. The results thus led to determinations of mean skin friction coefficients as functions of Reynolds Number. Tests were made at several different Mach Numbers in the low supersonic range. The range of Reynolds Numbers extended from 2×10^6 to 19×10^6, with corrections being made for the position of the effective leading edge of the plate as influenced by the presence of

a turbulence tripper strip near the physical leading edge. The range of Mach Numbers extended from $M_1 = 1.579$ to 2.471, these values being determined by the nozzle blocks available for the Ordnance Aerophysics Laboratory wind tunnel in which the tests were run. A set of blocks for $M_1 \cong 2.75$ was also available but was not used in the boundary layer program because of the relatively poor quality of the test section flow.

The results of these tests can be presented graphically in condensed form by making use of the analysis which led to Eq. (52). Thus Fig. 14 is a plot of X as a function of Y with the latter two quantities defined by Eqs. (49) and (50), respectively. According to Wilson's analysis, this plot should result in a single curve which is independent of Mach Number. The experimental values for each of the test values of Mach Number are indicated separately in Fig. 14 and very satisfactorily confirm the analysis which resulted in Eq. (52).

For engineering purposes and to minimize the amount of numerical computation required, the set of charts developed by Clutter and presented in Ref. (9) are probably to be preferred, since they yield directly the values of C_F for specified values of the Reynolds Number, with a separate chart being available for each Mach Number between $M_1 = 0$ (incompressible flow) and $M_1 = 5$. These charts also include the effects of sand-grain type roughness, represented by the ratio of the plate length ℓ, to the mean sand particle dimension k.

Wilson's measurements of velocity across the boundary layer were studied to only a limited extent in comparison with the velocity profiles predicted by the analysis. There were indications that pointed up the need for improved assumptions regarding the shear stress and mixing length distributions, but these points will not be discussed in detail in the present report since they do not

significantly alter the relationship between skin friction coefficient and Reynolds and Mach Numbers.

6.2 Skin Friction Measurements on Roughened Plates

The initial phase of the ARL investigation of roughness effects began as a natural extension of the smooth plate experiments, following lines comparable to those employed by Nikuradse in his studies of turbulent flow in pipes. The sand-grain type of surface was formed on the smooth plate by first coating it with a mixture of clear varnish and drier. The roughness itself was formed by applying grinding compound of various sizes to the plate with a flocking gun with care being taken to obtain as uniform a surface as possible. The results of these initial experiments on roughness are presented in a report by Shutts and Fenter [Ref. (29)], the tests being made in the OAL wind tunnel. The Reynolds Number range was from 4×10^6 to 2×10^7, while the Mach Number varied from 1.62 to 2.50 in increments of approximately 0.25. Several different sizes of grinding compound were utilized, the pertinent data being summarized in Table III.

A typical plot of mean skin friction coefficient as a function of Reynolds Number is shown for one Mach Number, $M_1 = 2.00$, in Fig. 15. Three values of the roughness parameter are included in this plot corresponding to values of $R_r = 0$, the smooth plate, and for $R_r = 2.59 \times 10^3$ and 4.01×10^3. The theoretical curves shown in Fig. 15 were based on Wilson's analysis of Ref. (7) in the case of the smooth surface, and on Fenter's treatment of uniformly rough surfaces as presented in Ref. (11).

The test program represented by Ref. (29) included boundary layer velocity surveys, as well as skin friction balance determinations of local shear stress. The latter values were integrated with respect to x, the distance along the plate, to obtain the values of the mean

skin friction coefficients shown in Fig. 15. A limited comparison of local skin friction coefficients with theory was presented, with agreement comparable to that obtained for the mean values.

Since these tests represented the first experience at ARL with roughened surfaces and with the use of the skin friction balance, it is considered significant to note some of the special problems resulting from the introductions of the grit-type of roughness and the balance measurements. The grit particles, when observed under a microscope, were extremely irregular in shape, so that a statistical approach was indicated to obtain the mean roughness dimension. For a given grit as many as 250 samples were observed microscopically and the average dimension of these samples used as a means of determining the value of r, the mean roughness dimension. In the case of the skin friction balance measurements on the roughened surface, it was necessary to use extra care to insure that roughness particles did not enter into the gap between the balance disk and the surrounding plate area. Such fouling would of course prevent the disk from experiencing the normal displacement to be expected from the action of the shear force.

Additional phases of the roughness program at ARL included extensions of the work reported on in Ref. (29), with particular attention being given to a comparison of the skin friction balance and Preston tube methods of determining local values of the skin friction coefficient. A special investigation was initiated to determine the equivalent roughness of surfaces having other than the grit type coating, which was accomplished by installing suitably machined inserts in a basic flat plate model. These tests were conducted in both the OAL and ARL wind tunnels. Another aspect of the program involved measurements on a cone-cylinder model in the supersonic wind tunnel of the Vought Aeronautics Division of Ling-Temco-Vought, Inc. The details of these various segments of the program were presented in a series of ARL reports, but the essential findings are well summarized in Ref. (11).

6.3 Skin Friction and Heat Transfer Measurements on Roughened Plates

The final phases of the ARL roughness effects program were extended to include measurements under heat transfer conditions. At the same time it was decided to standardize on a Veegroove type of roughness as being representative of machined surfaces resulting from actual production procedures. The initial work along these lines is covered in the report by Young [Ref. (12)] already cited in connection with the analytical studies. His experiments involved the addition to the plate of a coating of tin-lead solder, followed by a rolling process in which Veegrooves of the desired dimensions were impressed upon this coating. Since the basic plate model was fabricated of copper, considerable difficulty was experienced in attempting to machine such grooves into the plate itself. The rolling process applied to the solder coating appeared to avoid the galling that occurred with the machining procedure as indicated by microscopic examination of the completed surface.

The particular pattern of Veegrooves selected for this study had a 90 deg angle at the peak, so that the height of the projection was always one-half of the base width. The longitudinal axis of the grooves was perpendicular to the plate center line and the flow direction. While some degree of temperature elevation could be introduced into the wind tunnel air supply, provision was also made for internal cooling of the plate model so as to increase the range of the ratio of wall to free stream temperature. The internal cooling system was also designed so as to control the plate to a uniform temperature over its entire surface. The specific dimensions used in this series of experiments were roughness heights of 0.005, 0.010, and 0.030 in.

The instrumentation employed in the program had to meet the requirement of simultaneous measurements of local skin friction and of heat transfer rate. This objective was accomplished by providing two holes in the plate at a distance of 12.5 in. aft of the leading edge with centers located 1.0 in. on each side of the longitudinal center line. One of the two holes was designed to accommodate a floating element balance, while the other provided for the installation of a plug-type calorimeter. Both the balance shear disk and the calorimeter plug had diameters of 1.00 in. The nominal Mach Number of the wind tunnel air flow was 4.90, while the temperature ratio, T_w/T_1, ranged from about 5.2 to 2.9. Variations in this ratio could be obtained by adjusting the stagnation temperature of the tunnel air flow, the wall or surface temperature of the plate, or both. Heat transfer rates were determined by a transient method in which the surface temperature of the calorimeter plug was decreased abruptly by injection of about 10 cm^3 of cold water on its surface. The injection tube was then pulled up out of the main flow and the calorimeter and surrounding plate temperatures were recorded at frequent time intervals. The value of the Stanton Number was calculated on the basis of the temperature-time gradient at the instant when the calorimeter and plate temperatures were the same. In this manner any errors due to incomplete insulation of the calorimeter disk were minimized. The details of this procedure are fully described in Ref. (12).

The skin friction balance readings were taken simultaneously with the calorimeter readings, but the Pitot surveys across the boundary layer had to be made in separate runs. It should also be noted that the temperature ratios for the runs with the different degrees of roughness were not exactly the same throughout the series, due to difficulties in maintaining precise temperature control. Since all other parameters such as Reynolds Number, Mach Number, and degree of roughness were essentially constant, it would

have been preferable to interpret the data on the basis of variations in c_f and c_h with temperature ratio. Actually the test program was executed with a constant value of the plate temperature at $T_w = 555°R$ and the temperature ratio varied by adjusting the tunnel stagnation temperature and the ambient air temperature, T_1. This procedure led to variations in Reynolds Number with temperature ratio for a given measurement station, although this variation was not large.

A consideration of all of these factors finally brought the investigators to the conclusion that it was best to consider the local skin friction coefficient and the Stanton Number as functions of the roughness Reynolds Number, represented by

$$R_r = u^* k_r/2 \quad . \tag{103}$$

In addition to the data given in Ref. (12), involving Veegroove heights up to 0.030 in., results obtained by Mann [Ref. (30)] are also included in these plots, which are shown here in Figs. 16 and 17. The initial work of Young was found to carry the roughness height approximately to the so-called threshold value, and Mann's study was therefore undertaken in order to extend the roughness heights to larger values, specifically 0.060 in. and 0.090 in.

The plot of Fig. 16 shows the variation in local skin friction coefficient, c_f, with the roughness Reynolds Number R_r. Although not strictly correct, it is assumed that the temperature ratio is constant for each of the curves drawn. If the values of T_w/T_1 are considered as "standard" for the smooth plate runs, the percentage variation in temperature ratio in general does not exceed ±5%, although there are one or two cases of roughened plate where the variation was as high as 7 to 12%. Another factor involved in interpreting these results is based on the fact that the so-called "smooth plate" was undoubtedly not completely smooth in an aerodynamic sense. Thus while

the test values of c_f are plotted as corresponding to $R_r = 0$, the horizontal lines drawn through these points serve to indicate that they should be displaced slightly to the left. Profilograph measurements over a representative area of the smooth plate would have served to establish an appropriate value of k_r, but such equipment was not available for this purpose during the test program. A similar comment also applies to the heat transfer data shown in Fig. 17 in which the Stanton Number S is plotted against R_r.

In addition to the small variations in temperature ratio between one surface and another, a more significant factor should be noted, i.e., that there is a substantial variation in Reynolds Number between runs. Thus for the adiabatic wall condition, the nominal Reynolds Number is $R = 14 \times 10^6$, while for the runs at a temperature ratio $T_w/T_1 = 2.8$, the Reynolds Number has decreased to 5×10^6. Thus, Figs. 16 and 17 are really two parameter families of curves involving both temperature ratio and Reynolds Number as parameters. A more useful correlation of these measurements would have been obtained if the Reynolds Number had been maintained at a constant value while the temperature ratio was varied for a given degree of roughness. This would presumably require that the tunnel temperature be held constant and the temperature ratio be varied by means of the model cooling system. Such an approach might have resulted in severe restrictions on the range of temperature ratios that could be covered. The execution of such a test program in a continuous-flow rather than a blow-down wind tunnel would also be preferable, since once a stable flow was established in the tunnel, the temperature ratio could then be varied systematically during a single run without interruption.

Using the data shown in Figs. 16 and 17, values of the Reynolds Analogy factor, p, as defined by Eq. (97), were computed and plotted as functions of temperature ratio in Fig. 18. While

rough mean curves could be drawn through the data points for each of the different roughness values, the extreme scatter of the data made it undesirable to do this. Also such curves seem to exhibit no logical or systematic trends with increasing roughness. The remedy for this situation is undoubtedly to be found in the more elaborate test procedure outlined above, particularly one involving more precise control of all flow parameters as well as the plate temperature. Similar results are given in a technical journal paper by Young and Westkaemper [Ref. (31)] but based only on the initial group of roughness values reported on in Ref. (12).

As mentioned earlier in connection with the outline of Young's research program, his experimental work also included Pitot probe surveys of the velocity distribution across the boundary layer. These results were expressed initially in terms of the velocity ratio, u/u_1, as a function of the normal distance y from the plate surface. Curves for the smooth plate and the different degrees of roughness are shown in Fig. 19 for the case of the insulated plate, that is, $T_w = T_{ad}$ or $T_w/T_1 = 5.2$. The data for the smooth plate and for $k_r \neq 0$ are so close together that only the curve for the smooth case is shown. The other cases show a steepening of the velocity gradient near the wall with increasing roughness which of course is consistent with the expected increase in skin friction shear stress. A second plot for $T_w/T_1 = 3.8$ is shown in Fig. 20 and indicates little change due to the change in thermal conditions. In both cases the free stream Mach Number was the usual value of $M_1 = 4.93$. These velocity measurements may be readily transformed into the usual semilogarithmic plots with u/u^* plotted as a function of $u^*y/2$; such a plot for $T_w/T_1 = 3.8$ is shown in Figs. 20 and 21 for the two cases just mentioned. In this form the effect of roughness is more readily apparent but the data are so irregular in character that no firm conclusions can be drawn from them as to the precise magnitude of the change. Again it would appear that

there is a real need for experiments in a continuous-flow wind tunnel under more precise control of temperature. One would hope that such experiments, when repeated, would lead to quantitative data on roughness effects comparable to Nikuradse's work on low speed pipe flow.

Although this report was prepared primarily as a summary of the ARL contributions to the turbulent boundary problem, including roughness and heat transfer effects, an effort has been made throughout to introduce references to other significant work in this area of recent date. In this connection the present report might be closed with a reference to a Symposium on Compressible Turbulent Boundary Layers held at the NASA Langley Research Center in December 1968 [Ref. (32)]. The Proceedings of this meeting provide a state-of-the-art summary for compressible flow comparable in many respects to the earlier Stanford report on incompressible flow. In both cases there appears to be a vigorous battle being waged between two schools of thought, first, those who favor the continued use of integral methods for the prediction of skin friction and heat transfer rates, and second, those who advocate a return to a more fundamental approach which might eventually lead to more rational theories. The large amount of empiricism involved in the first method is one of the major factors in limiting the usefulness of the integral approach. Carefully planned and conducted experiments on turbulent boundary layers in all aspects of the speed spectrum would do much to provide a sounder physical basis for analysis than that now available.

TABLE I

ROUGHNESS FUNCTION PARAMETERS

Range	η_r - Lwr.	η_r - Upr.	a	b
Smooth	0	5	0	0
Transition	5	100	2.84	4.58
Rough	100	---	2.50	3.00

TABLE II

THE NUMERICAL REPRESENTATION OF THE LAW OF THE WALL AND THE LAW OF THE WAKE AS DEVELOPED BY COLES [REF. (3)]

The Law of the Wall

η	$f_1(\eta)$
0	0
1	0.99
2	1.96
3	2.90
4	3.80
5	4.65
6	5.45
7	6.19
8	6.87
9	7.49
10	8.05
12	9.00
14	9.76
16	10.40
18	10.97
20	11.49
24	12.34
28	12.99
32	13.48
36	13.88
40	14.22
44	14.51
50	14.87
60	15.33
80	16.04
100	16.60
150	17.61
200	18.33
300	19.34
400	20.06
500	20.62
600	21.08
800	21.79
1000	22.35
1500	23.36
2000	24.08
3000	25.09
4000	25.81
5000	26.37
6000	26.83
8000	27.54
10000	28.10

The Law of the Wake

y/δ	$f_2(y/\delta)$
0.010	14.31
0.015	13.30
0.020	12.58
0.025	12.02
0.030	11.57
0.040	10.85
0.050	10.29
0.060	9.83
0.080	9.11
0.100	8.56
0.150	7.54
0.200	6.70
0.250	6.00
0.300	5.37
0.350	4.79
0.400	4.25
0.450	3.73
0.500	3.23
0.550	2.76
0.600	2.31
0.650	1.89
0.700	1.50
0.750	1.14
0.800	0.82
0.850	0.53
0.900	0.29
0.950	0.10
1.000	0

TABLE III

TEMPERATURE RATIOS AND ROUGHNESS HEIGHTS

Surface	$\frac{T_w}{T_1}$	T_1	T_{aw} deg R	To	$\Delta \frac{T_w}{T_1}$	$\frac{\Delta(T_w/T_1)}{(T_w/T_1)}$ smooth
Smcoth	5.186	104	591	607		
"	3.779	141.6	739	824.2		
"	3.503	153.6	799	894.1		
"	3.166	170.9	905	994.8		
"	2.782	197.3	1021	1148.4	4	
0.005	5.089	109.1	558	643.7	-0.097	-0.0187
"	4.030	138.0	724	814.2	+0.251	+0.0665
"	3.649	153.7	810	906.8	+0.146	+0.0417
"	3.240	174.7	913	1030.7	+0.074	+0.0234
"	2.993	190.1	999	1121.5	+0.211	+0.0731
0.010	5.171	105.4	544	620.0	-0.015	-0.00289
"	3.966	135.7	706	798.2	+0.187	+0.0495
"	3.597	152.1	796	894.7	+0.411	+0.1172
"	3.210	170.4	891	1002.4	+0.044	+0.0139
"	2.915	191.8	1004	1128.2	+0.133	0.0461
0.030	5.211	102.9	536	607.1	+0.025	+0.00482
"	3.754	144.9	771	854.9	-0.015	-0.00397
"	3.530	154.1	815	909.1	+0.027	+0.0077
"	3.206	170.3	899	1004.7	+0.040	0.01265
"	2.916	190.0	1006	1120.9	+0.134	0.0465

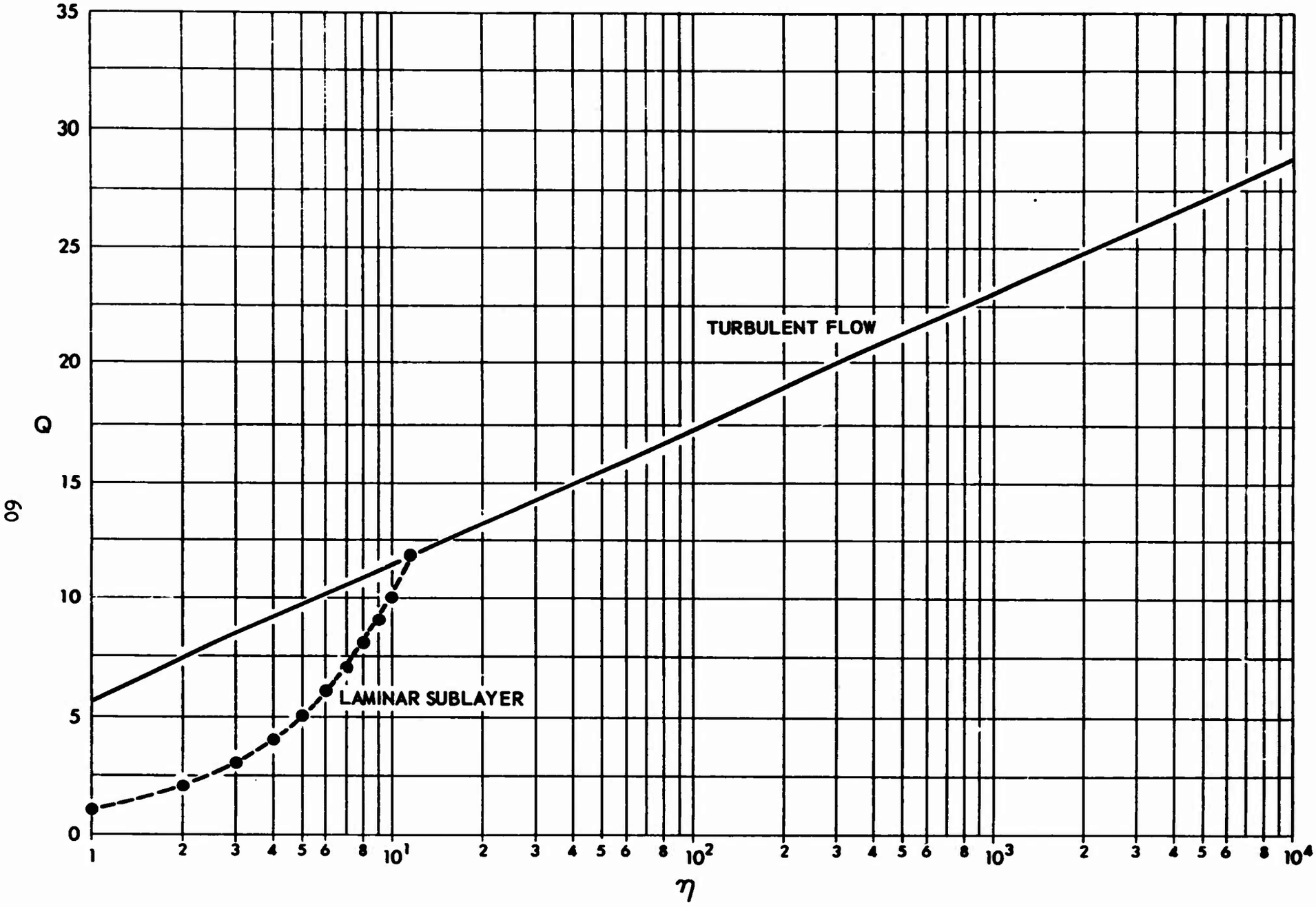

ARL : UT
AA-71-1
MJT - RFO
1-8-71

FIGURE 1
THE LAW OF THE WALL FOR INCOMPRESSIBLE FLOW

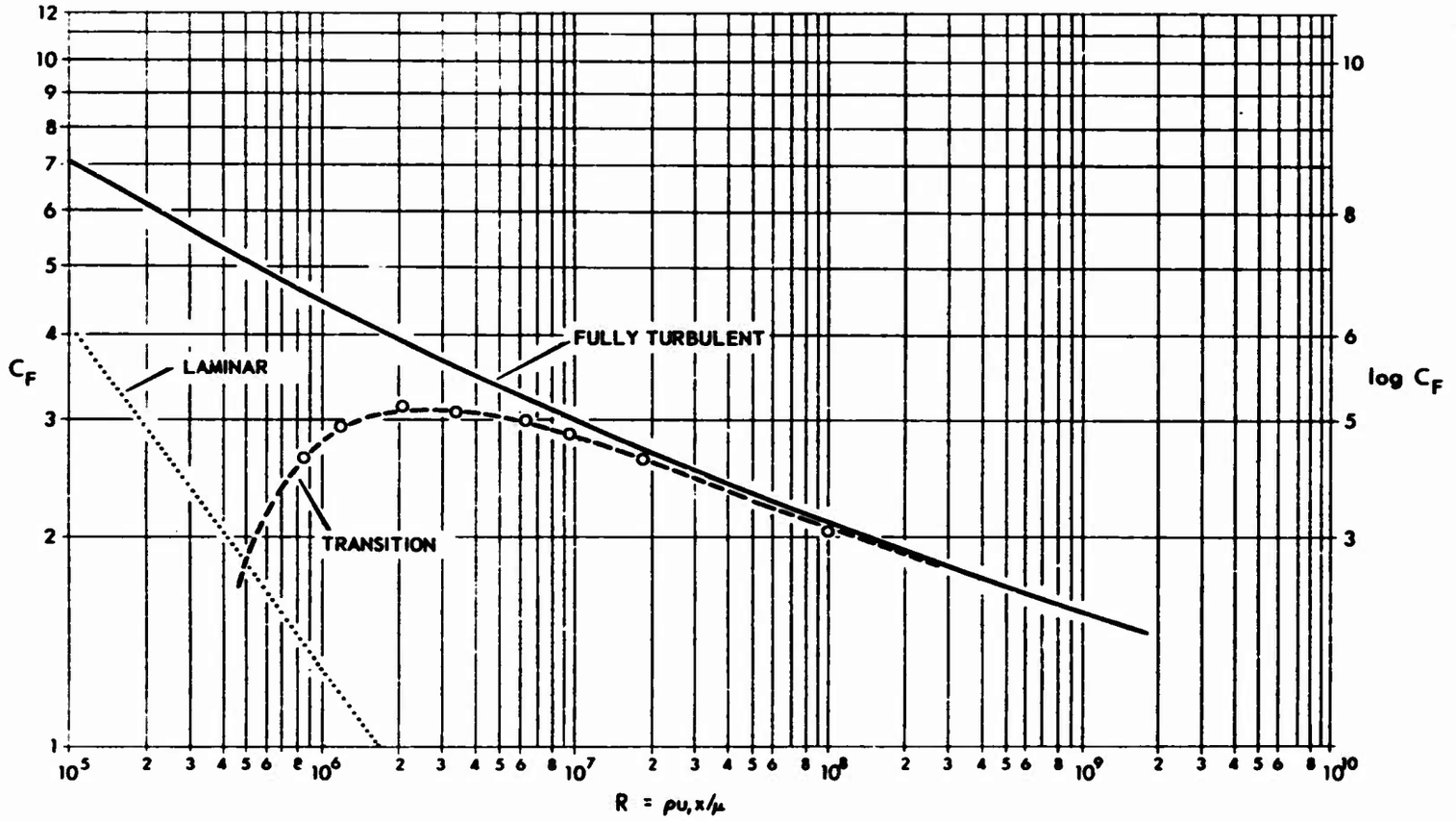

ARL - UT
AA-71 - 2
MJT - RFO
1-7-71

FIGURE 2
MEAN SKIN FRICTION COEFFICIENT vs
REYNOLDS NUMBER – INCOMPRESSIBLE FLOW

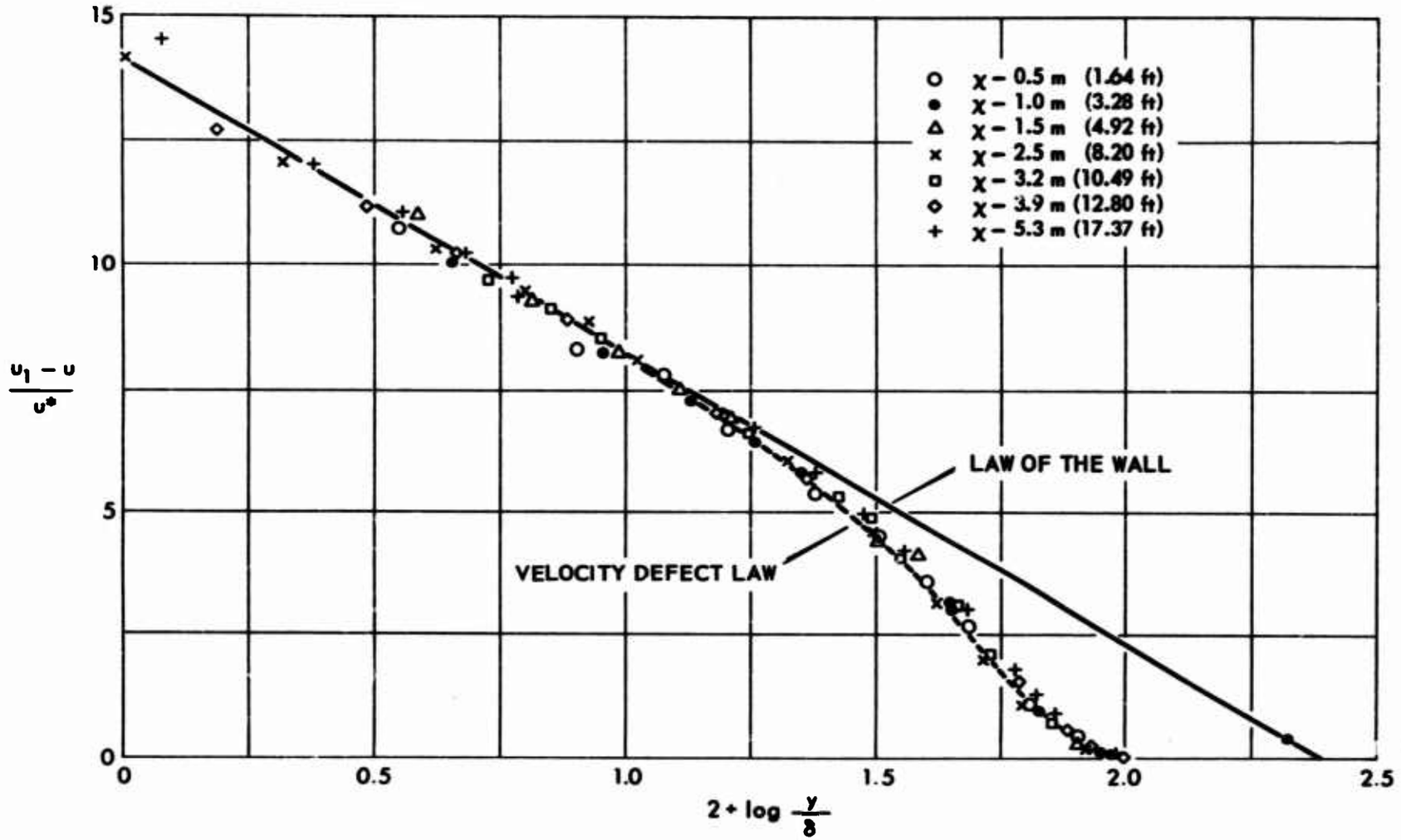

FIGURE REPRINTED FROM
NACA TECHNICAL MEMORANDUM No. 986

ARL - UT
AA-71-3
MJT - RFO
1 - 8 - 71

FIGURE 3
VELOCITY PROFILES ON A FLAT PLATE

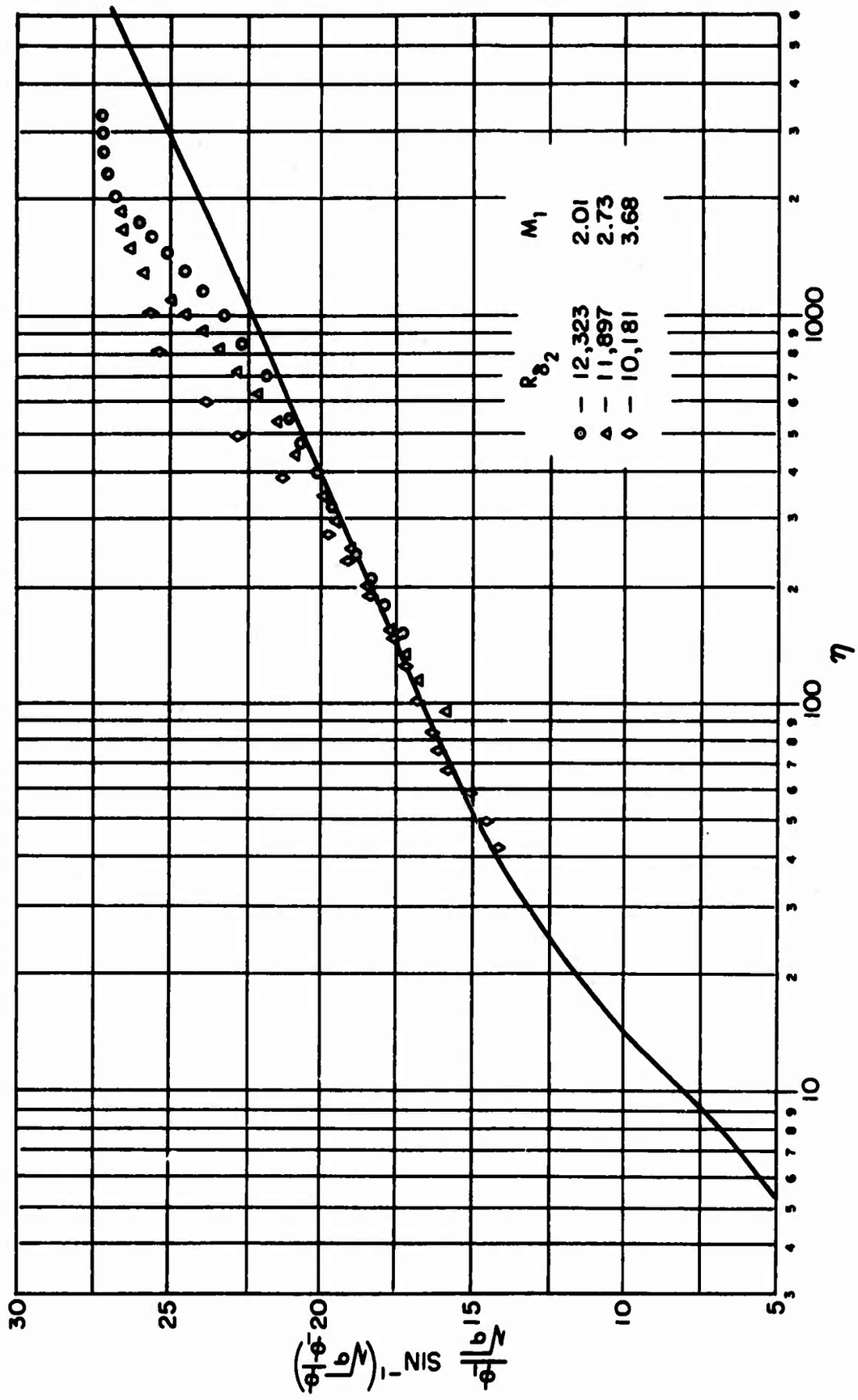

FIGURE 4
LAW OF THE WALL FOR COMPRESSIBLE FLOW

DRL – UT
DWG AA 2113
CJS – CLW
11 – 12 – 57

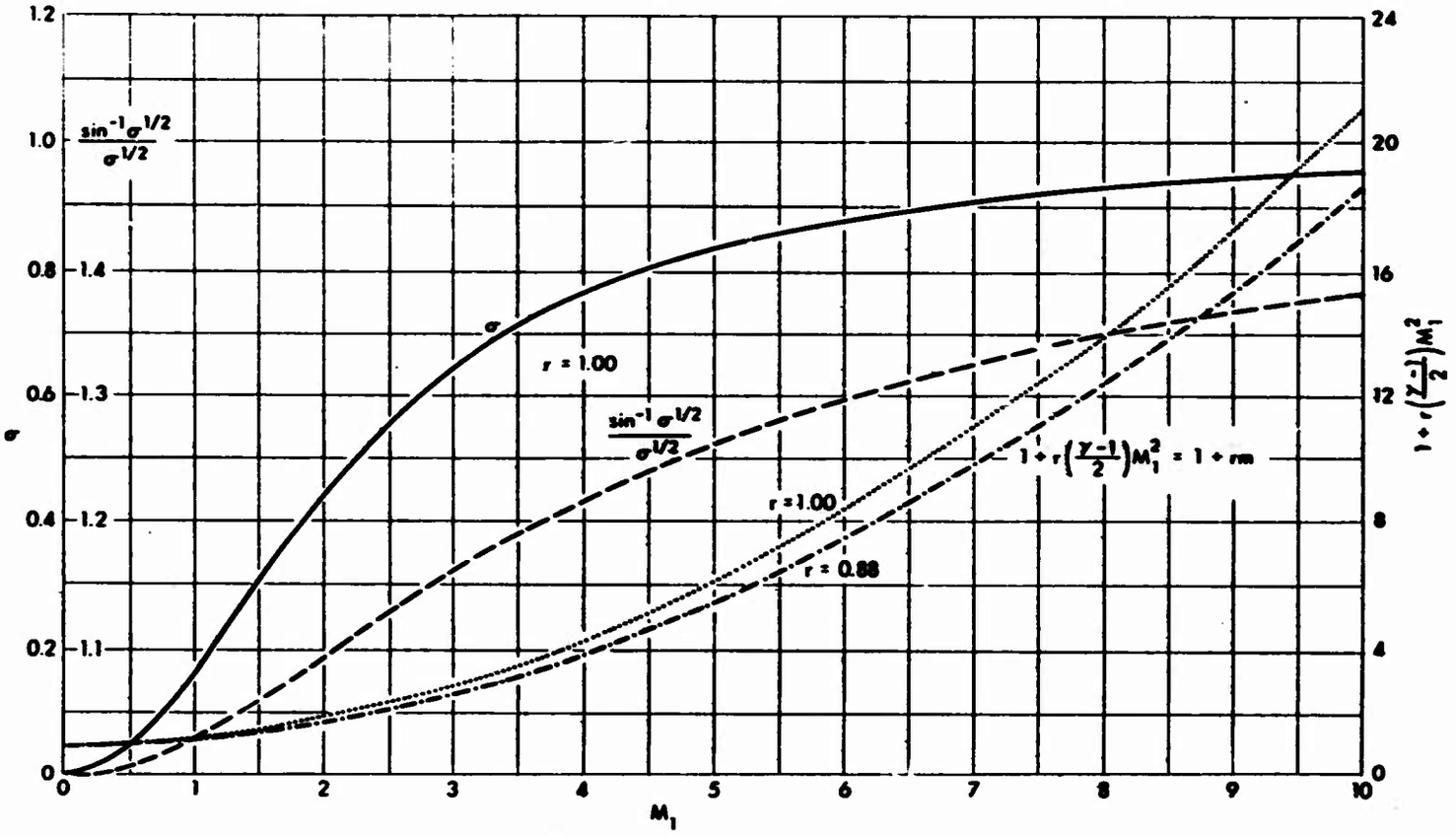

ARL - UT
AA-71-4
AUT - RFO
1 - 6 - 71

FIGURE 5
MACH NUMBER PARAMETERS FOR COMPRESSIBLE FLOW

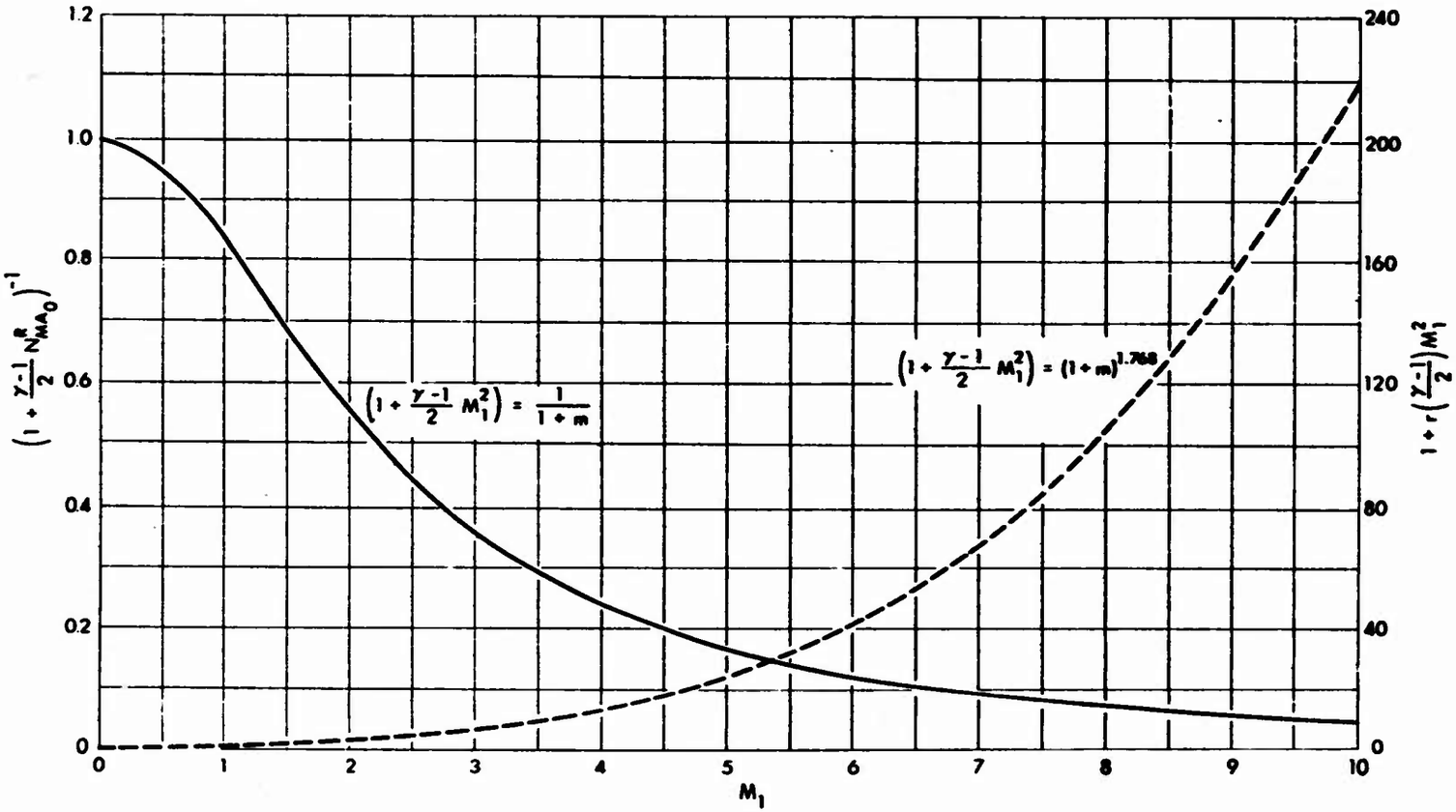

ARL - UT
AA-71-5
MJT - RFO
1-8-71

FIGURE 6
MACH NUMBER PARAMETERS FOR COMPRESSIBLE FLOW
WILSON'S THEORY – r = 1.00; ω = 0.768

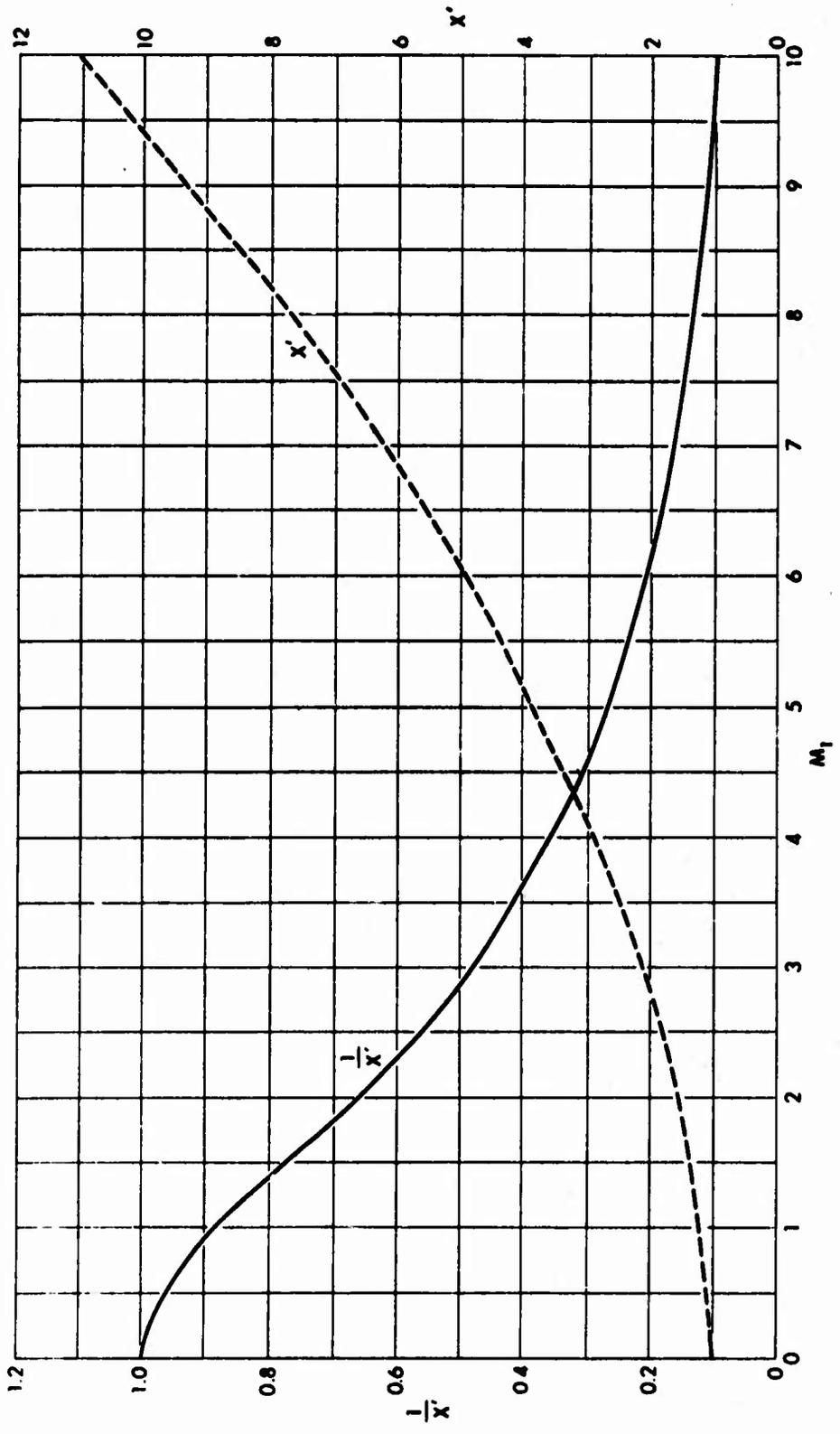

FIGURE 7
X' AND 1/X' vs M_1
WILSON'S THEORY – r = 1.00

ARL - UT
AA-7146
MJT - RFO
1-8-71

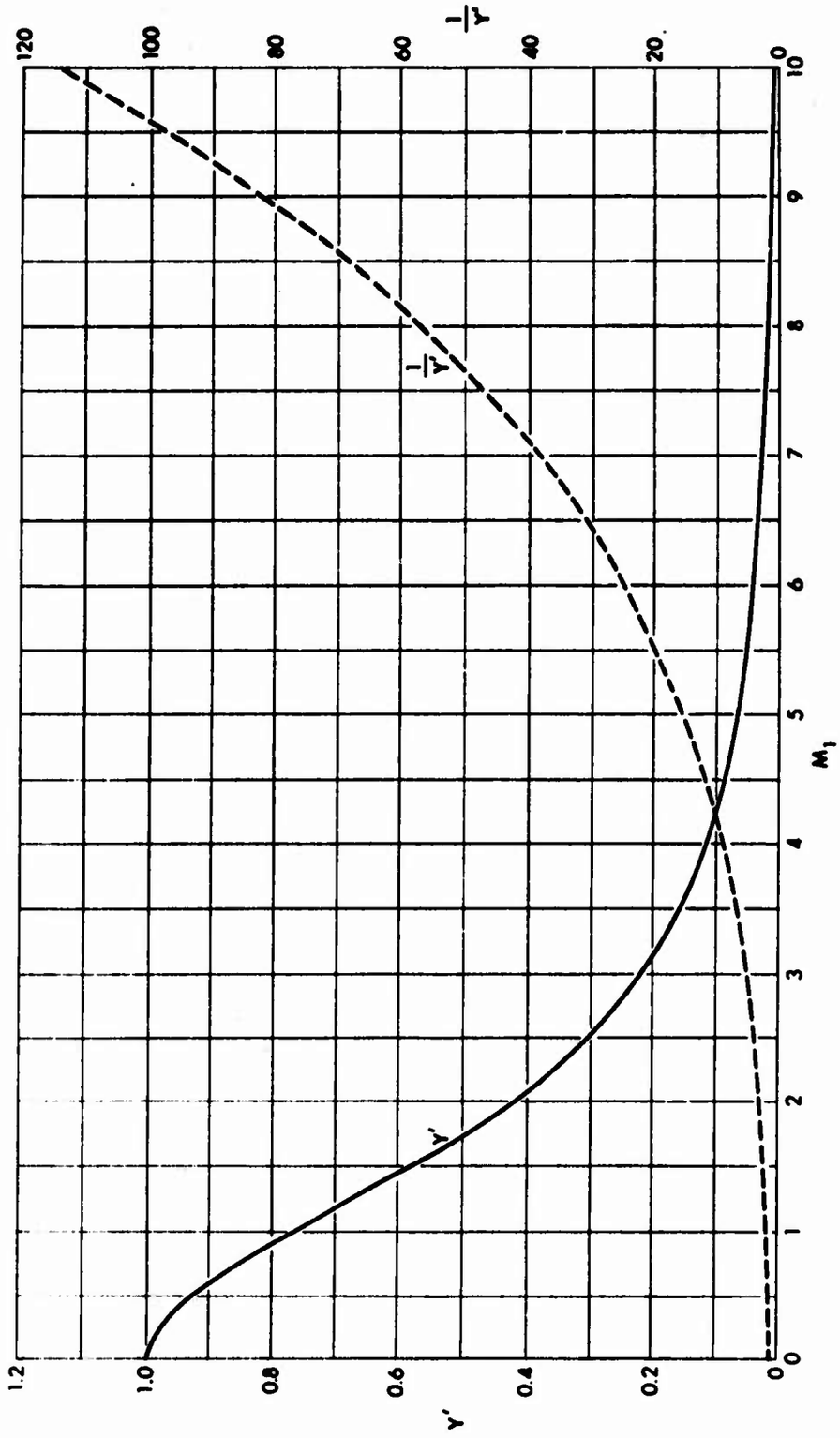

FIGURE 8
Y' AND 1/Y' vs M_1
WILSON'S THEORY -- r = 1.00

ARL - UT
AA-71-7
MJT - RFO
1-8-71

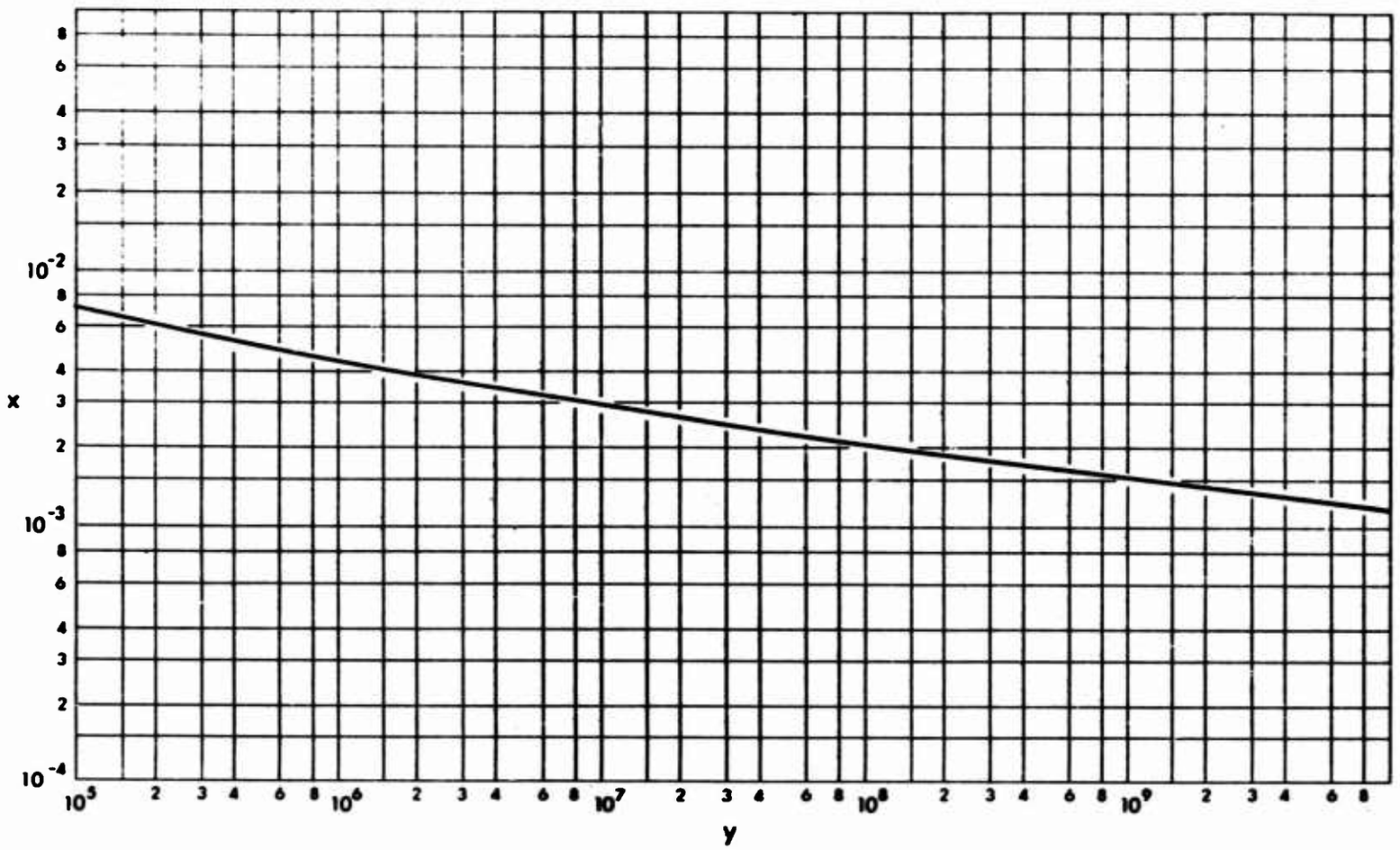

ARL-UT
AA-71-8
MJT-RFO
1-8-71

FIGURE 9
UNIVERSAL SKIN FRICTION REYNOLDS NUMBER RELATION FOR COMPRESSIBLE FLOW
WILSON'S THEORY – r = 1.00

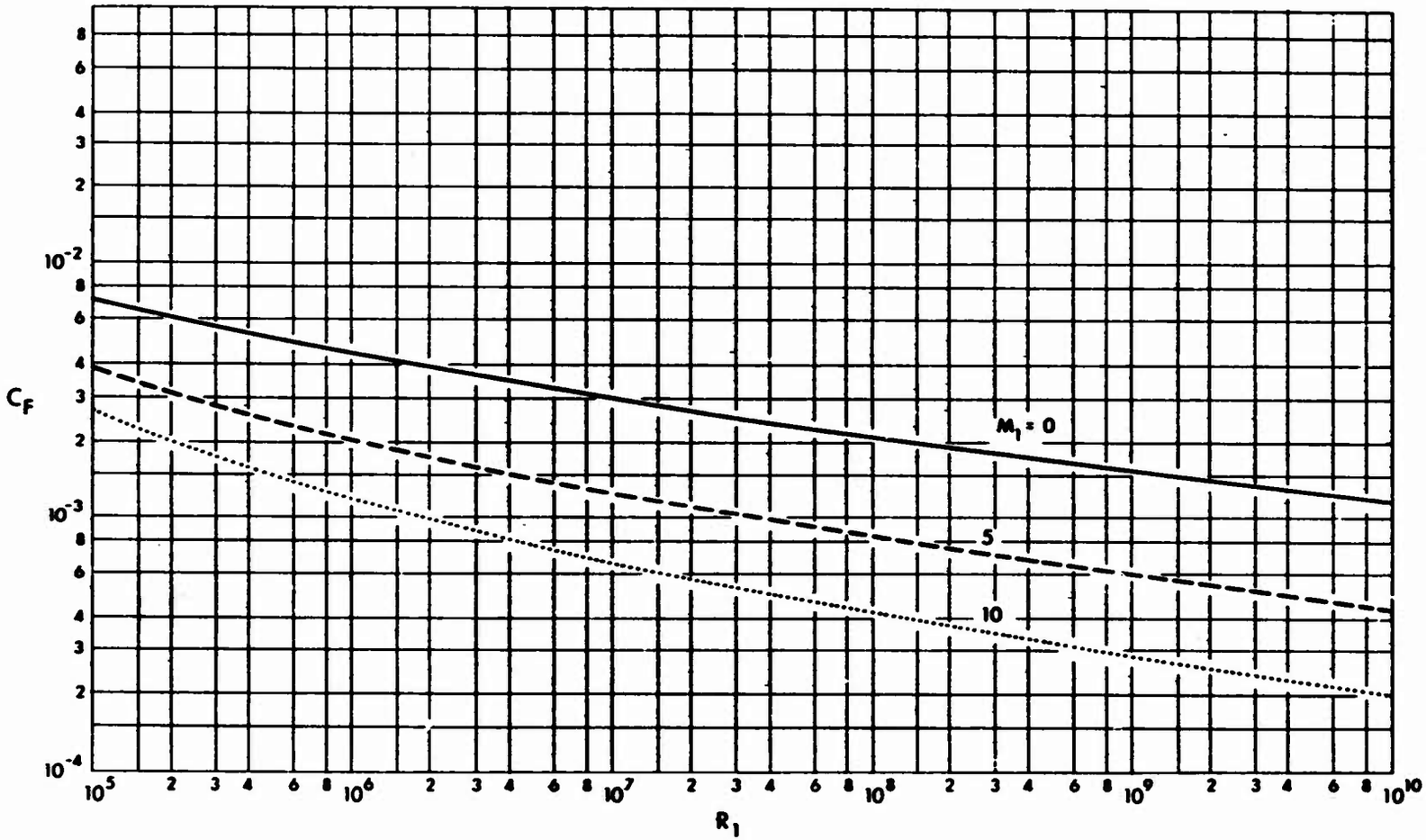

ARL - UT
AA-71-9
MJT - RFO
1-8-71

FIGURE 10
MEAN SKIN FRICTION COEFFICIENT vs REYNOLDS NUMBER
COMPRESSIBLE FLOW ON A SMOOTH ADIABATIC WALL
WILSON'S THEORY

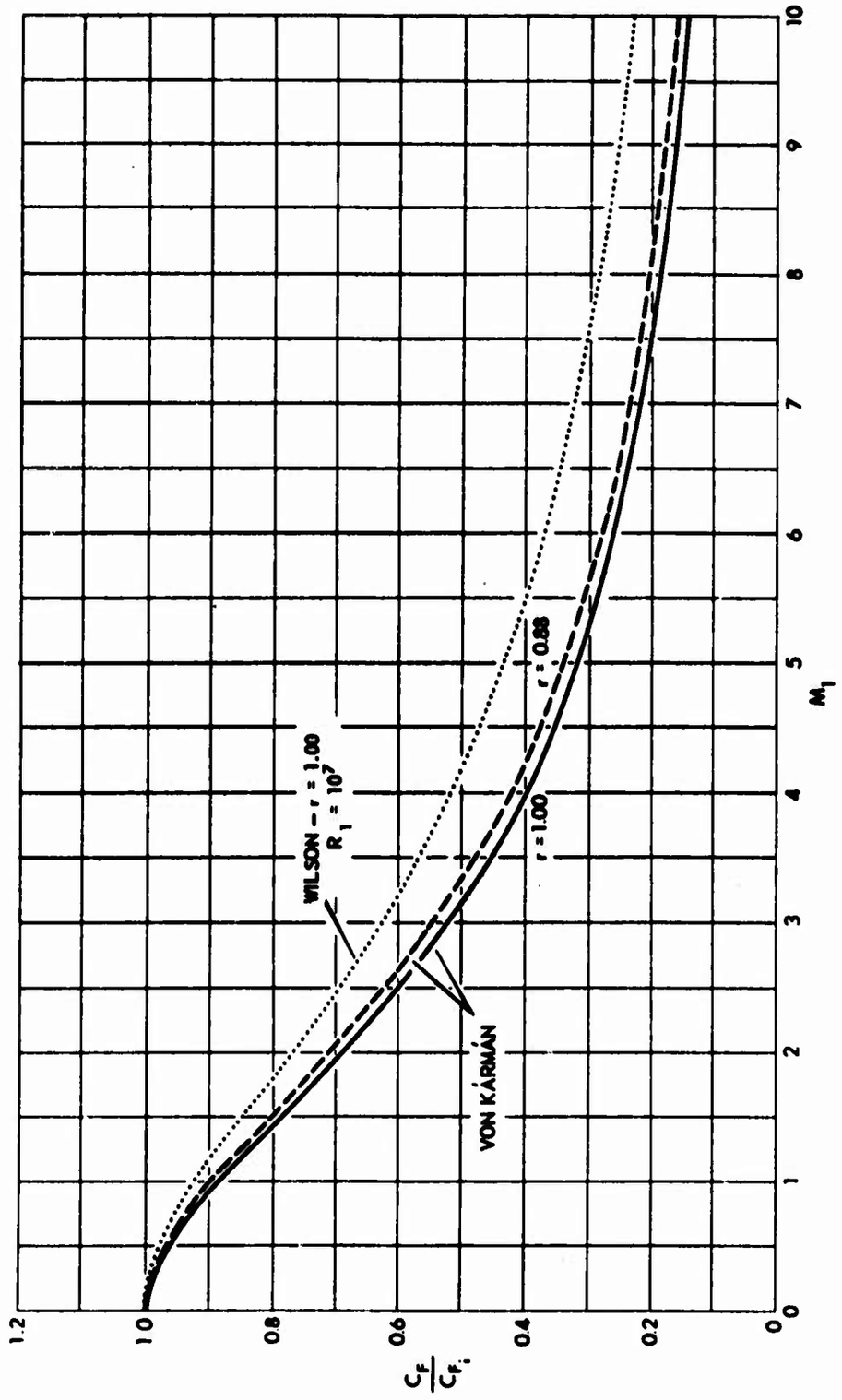

FIGURE 11
C_F/C_{F_i} vs MACH NUMBER

ARL - UT
AA-71-10
MJT - RFO
1-8-71

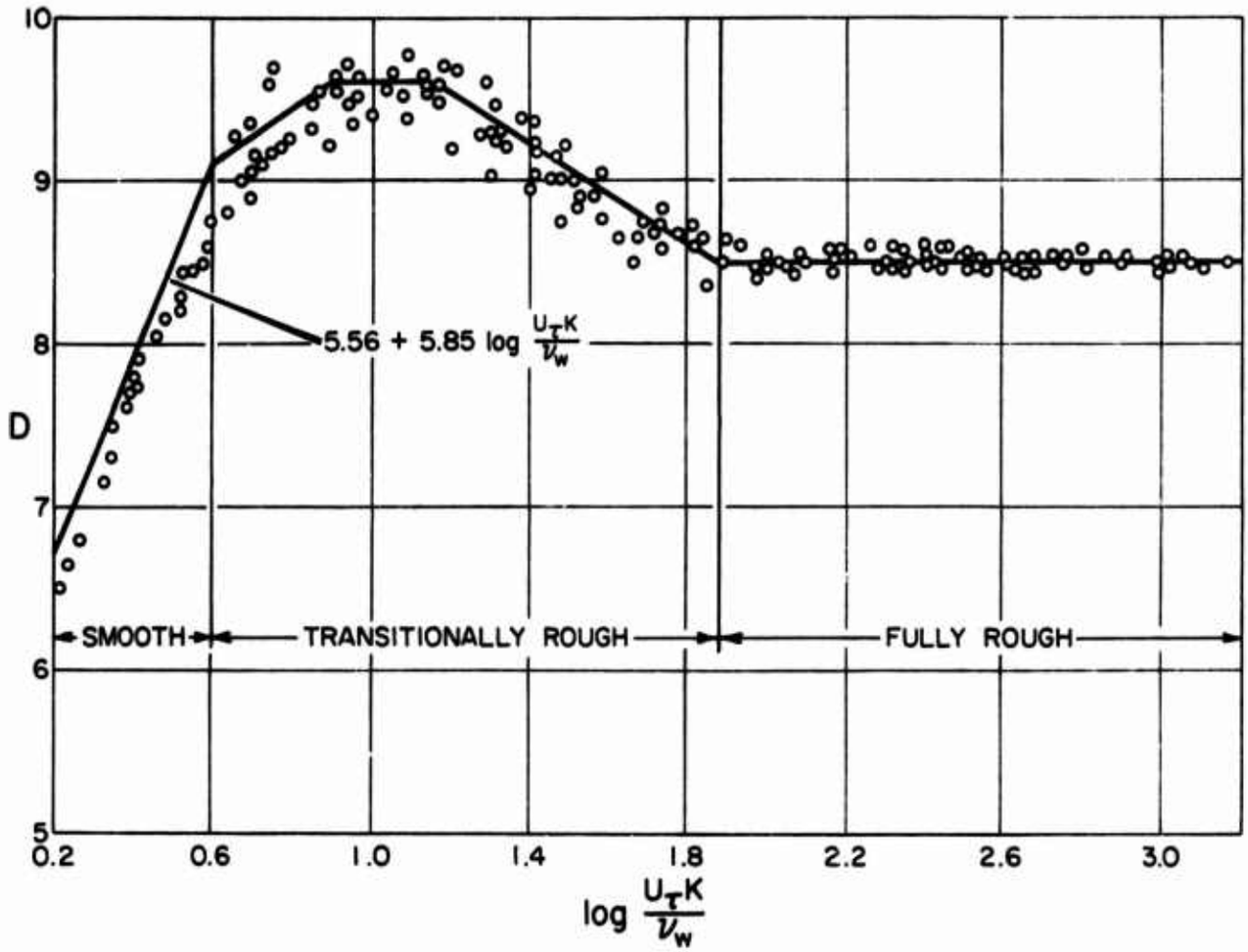

FIGURE 12
VARIATION IN ROUGHNESS FUNCTION
WITH ROUGHNESS REYNOLDS NUMBER

DRL - UT
DWG AA-65-2
FLY - EJW
4 - 2 - 65

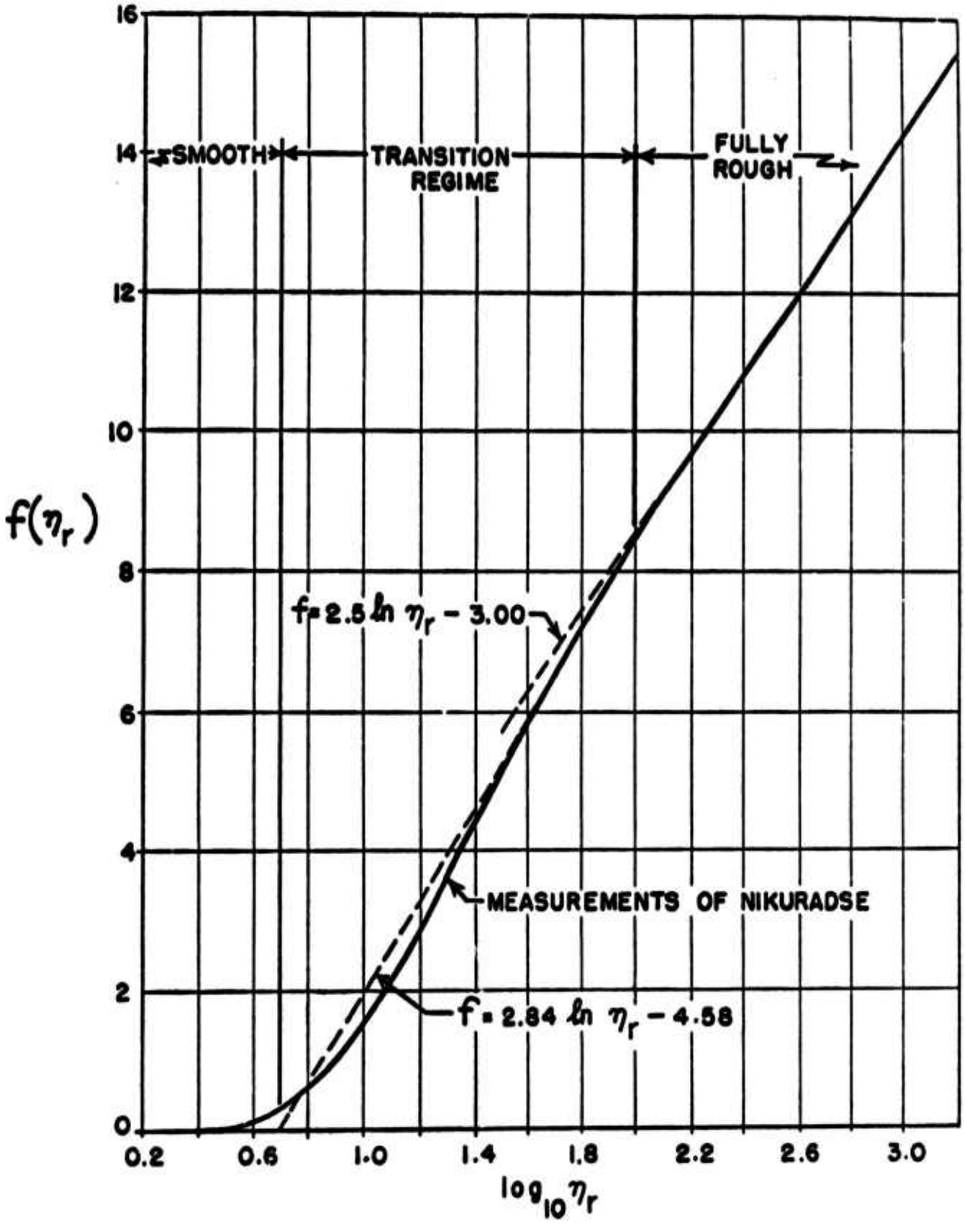

FIGURE 13

MODIFIED ROUGHNESS FUNCTION FOR IMCOMPRESSIBLE FLOW IN PIPES

DRL - UT
DWG
MJT - BEE
3 - 13 - 63

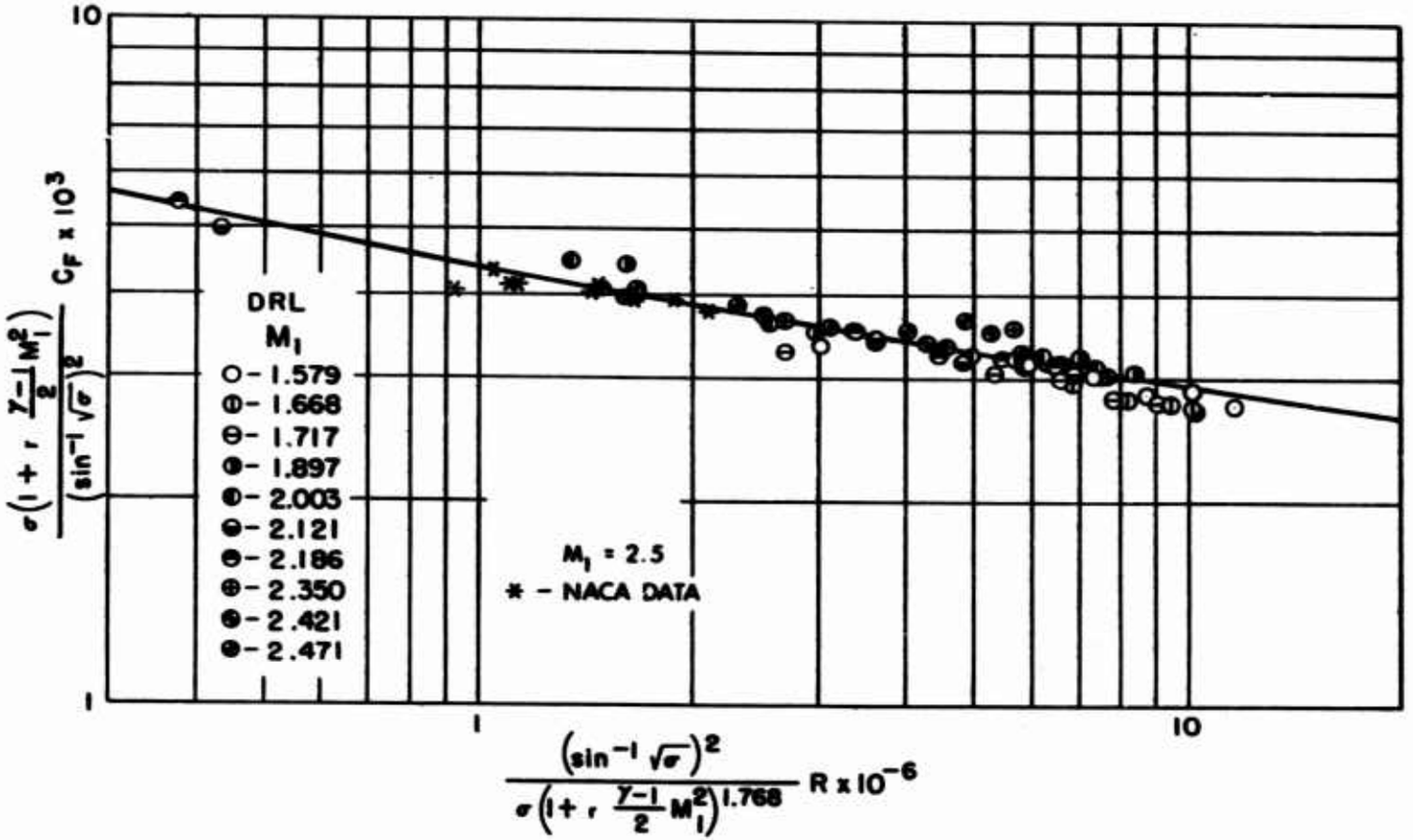

FIGURE 14
MEAN TURBULENT SKIN FRICTION COEFFICIENT
-SUMMARY – THEORY AND EXPERIMENT-

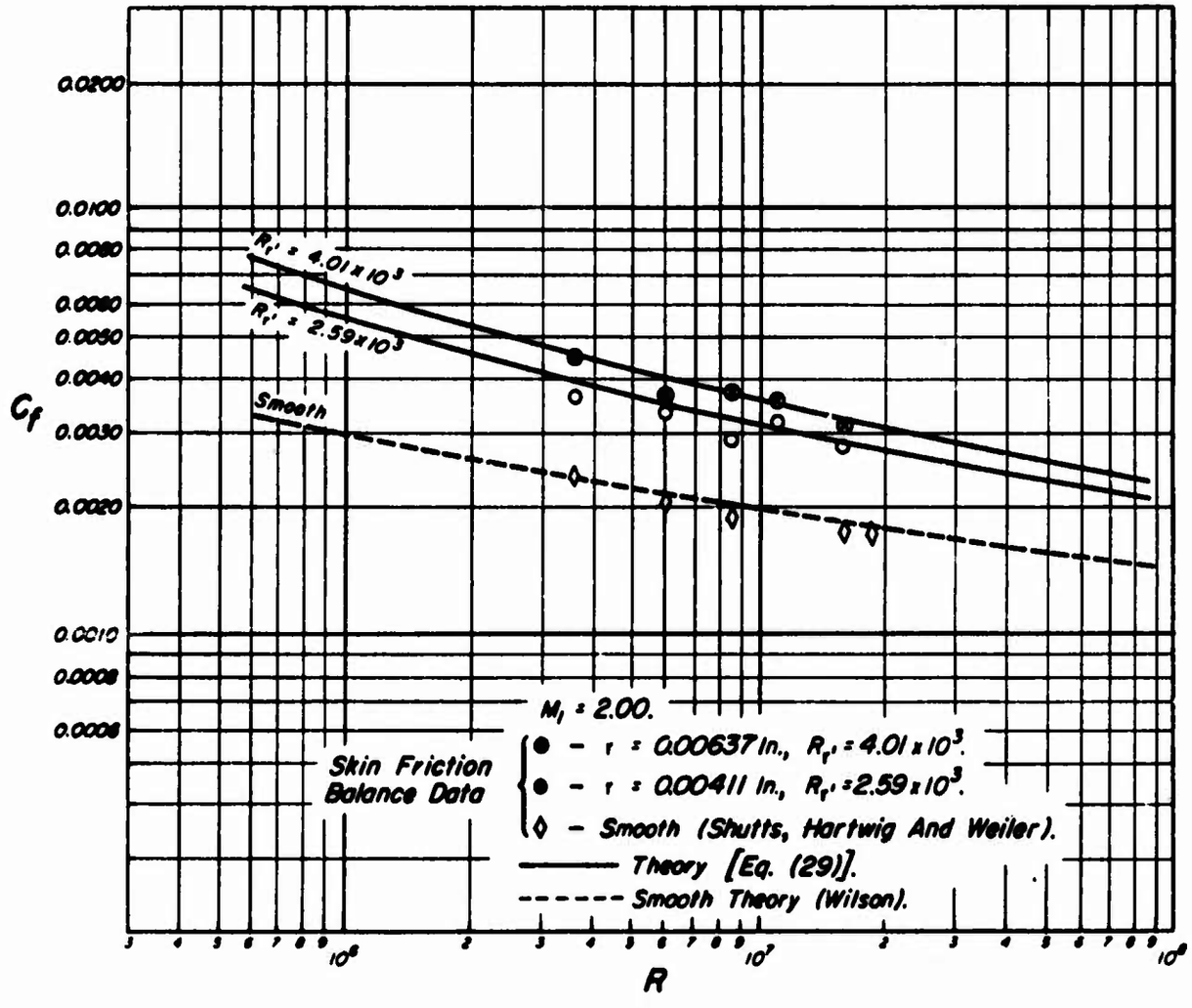

FIGURE 15
COMPARISON OF THEORY AND EXPERIMENT FOR
ROUGH, INSULATED PLATES AT $M_1 = 2.00$

DRL – UT
DWG AA 1510
FWF – EJW
2-23-56

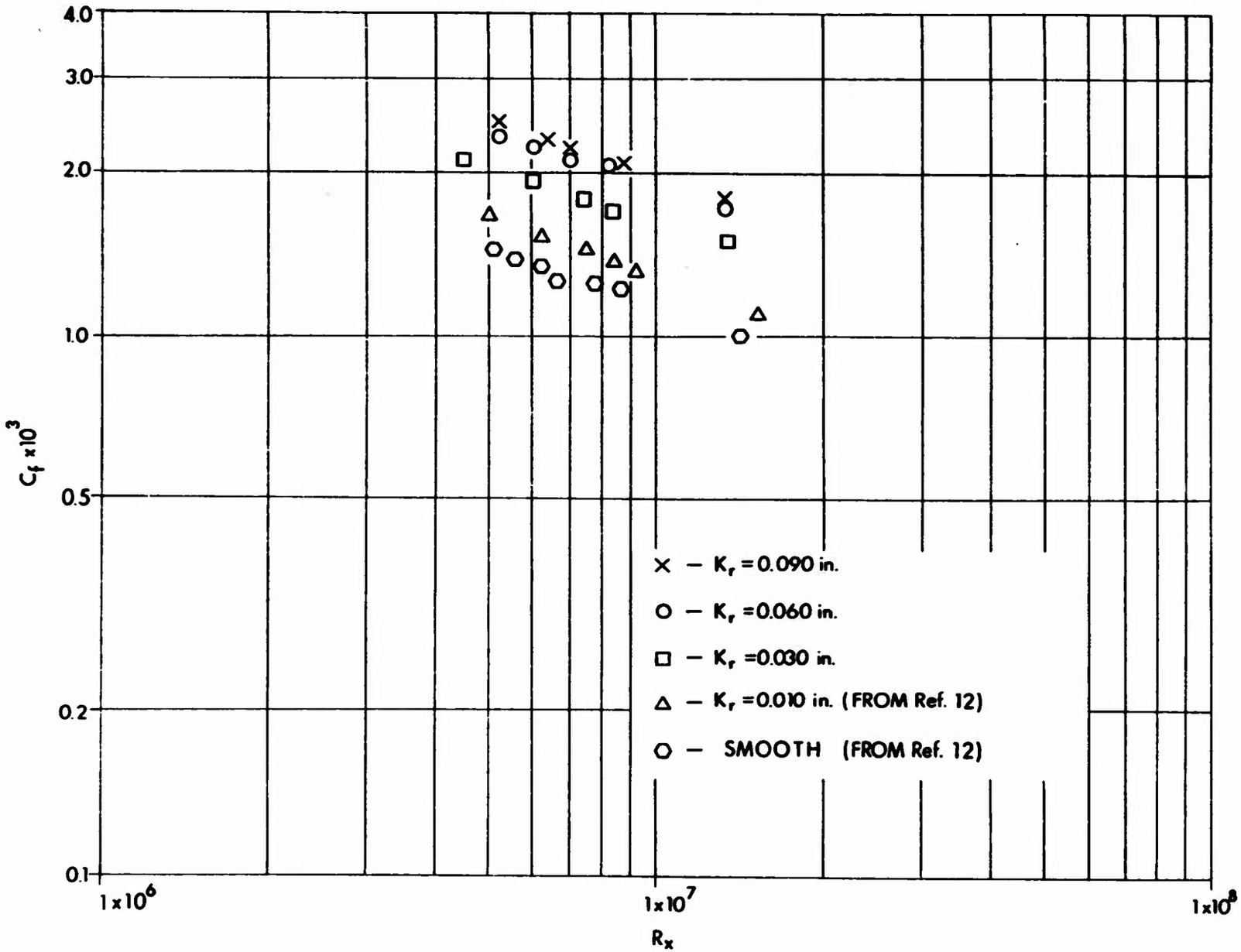

FIGURE 16
VARIATION OF EXPERIMENTAL LOCAL SKIN FRICTION COEFFICIENTS WITH REYNOLDS NUMBER AT $M_1 = 4.90$

DRL - UT
AA-67-20
HWM - JPB
8 - 28 - 67
181471

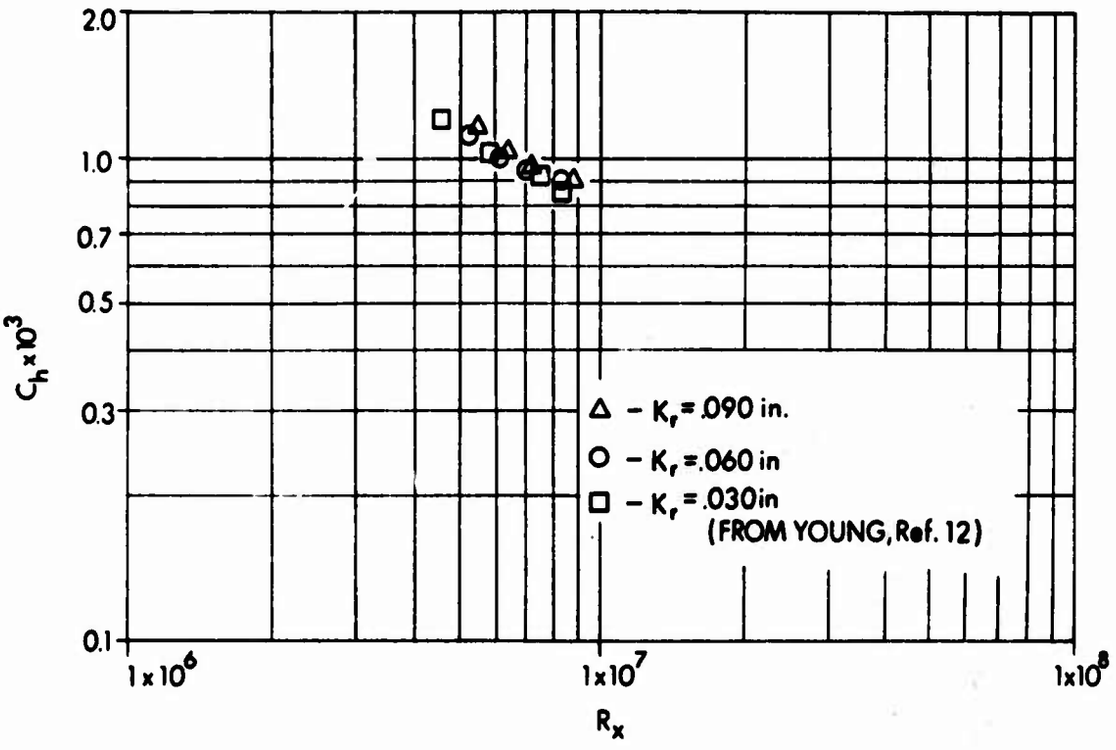

FIGURE 17
EXPERIMENTAL LOCAL STANTON NUMBERS
FOR SMOOTH AND ROUGH PLATES AT M_1 = 4.90

DRL - UT
AA-67-29
HWM - JPB
8 - 28 - 67
181471

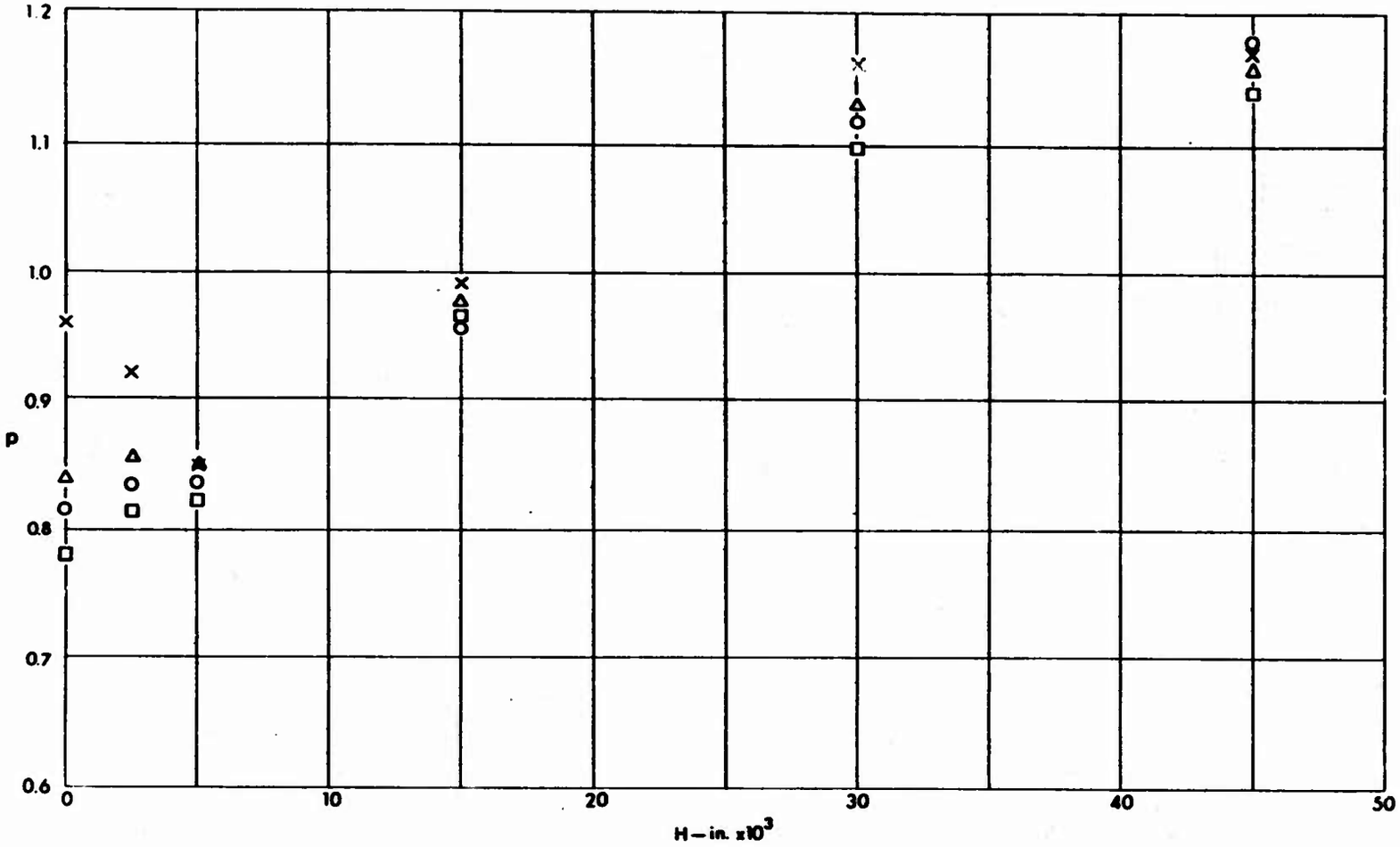

DRL - UT
AA-67-32
HWN - JPB
8-28-67
161471

FIGURE 18
THE EFFECT OF ROUGHNESS HEIGHT, H, ON EXPERIMENTAL REYNOLDS ANALOGY FACTORS FOR A FLAT PLATE AT M_1 = 4.90
(VALUES OF K_r = 0, 0.0025, 0.0050, 0.0150 in. TAKEN FROM YOUNG [Ref. (12)])

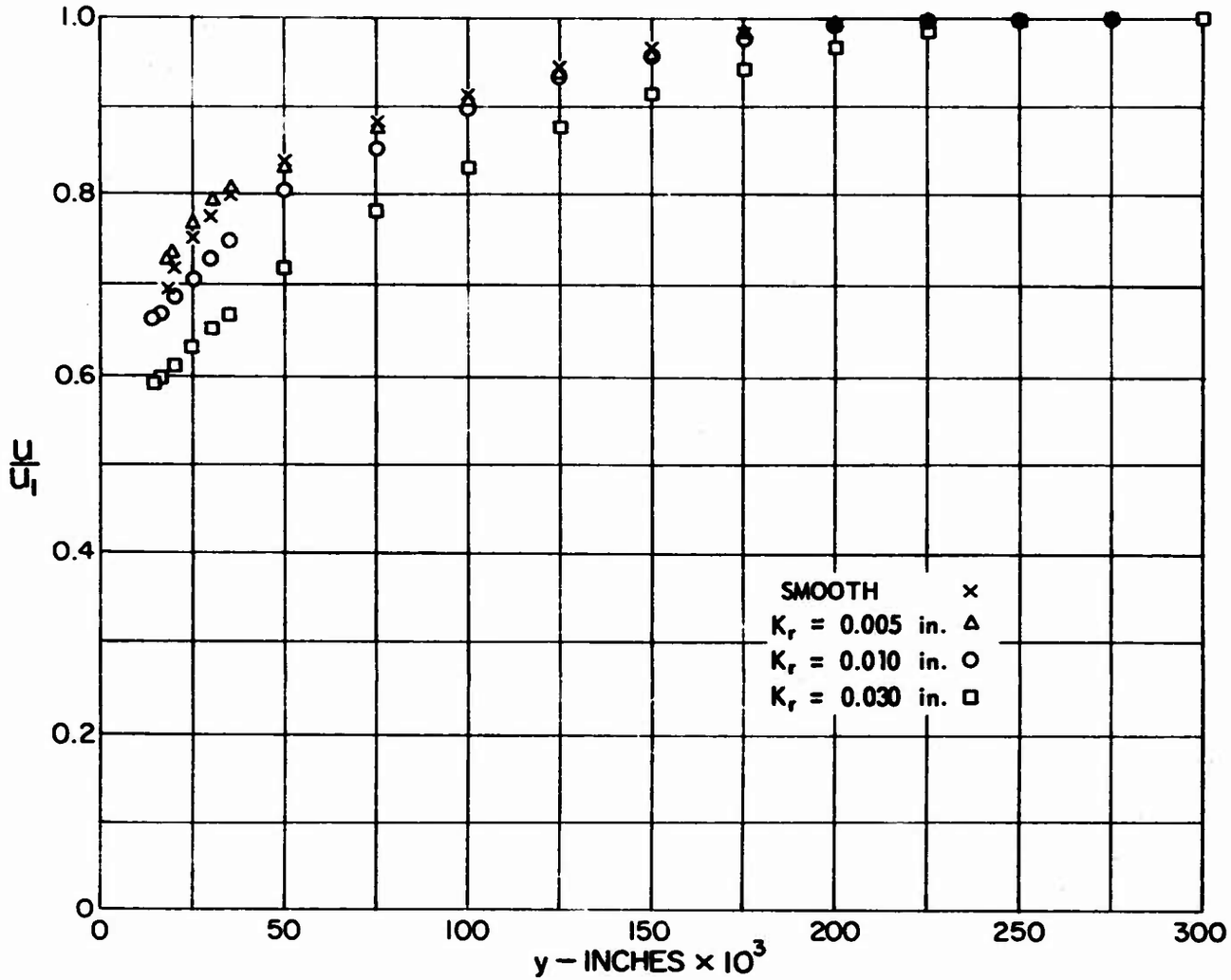

FIGURE 19
VELOCITY RATIO vs DISTANCE FROM THE
PLATE SURFACE FOR VARIOUS DEGREES OF ROUGHNESS
$M_1 = 4.93 \quad T_w = T_{ad} \quad T_w/T_1 = 5.2$

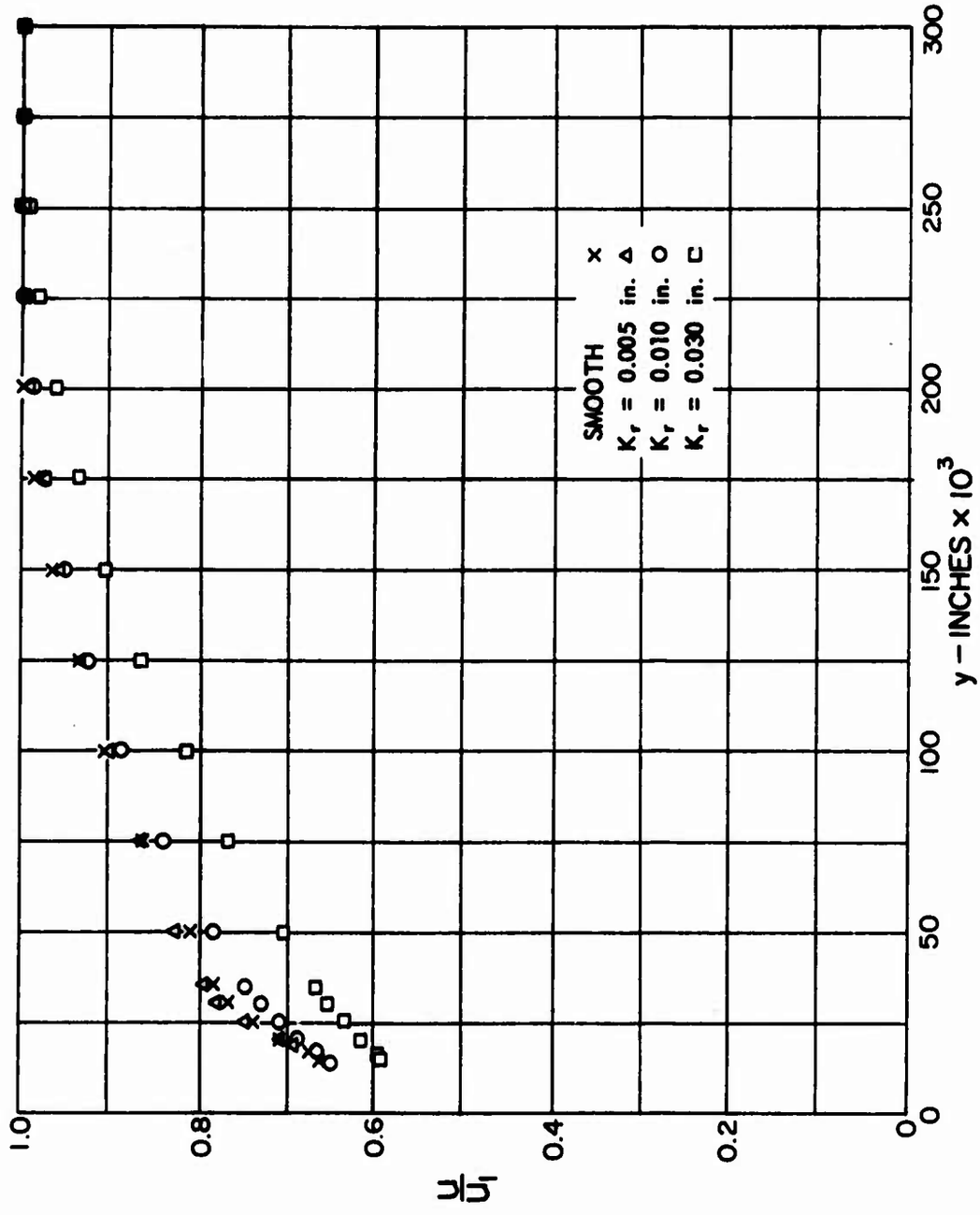

FIGURE 20
VELOCITY RATIO vs DISTANCE FROM THE PLATE SURFACE
FOR VARIOUS DEGREES OF ROUGHNESS
M_1 = 4.93, T_w/T_1 = 3.8

DRL - UT
DWG AA-65-17
FLY - EJW
4 - 2 - 65

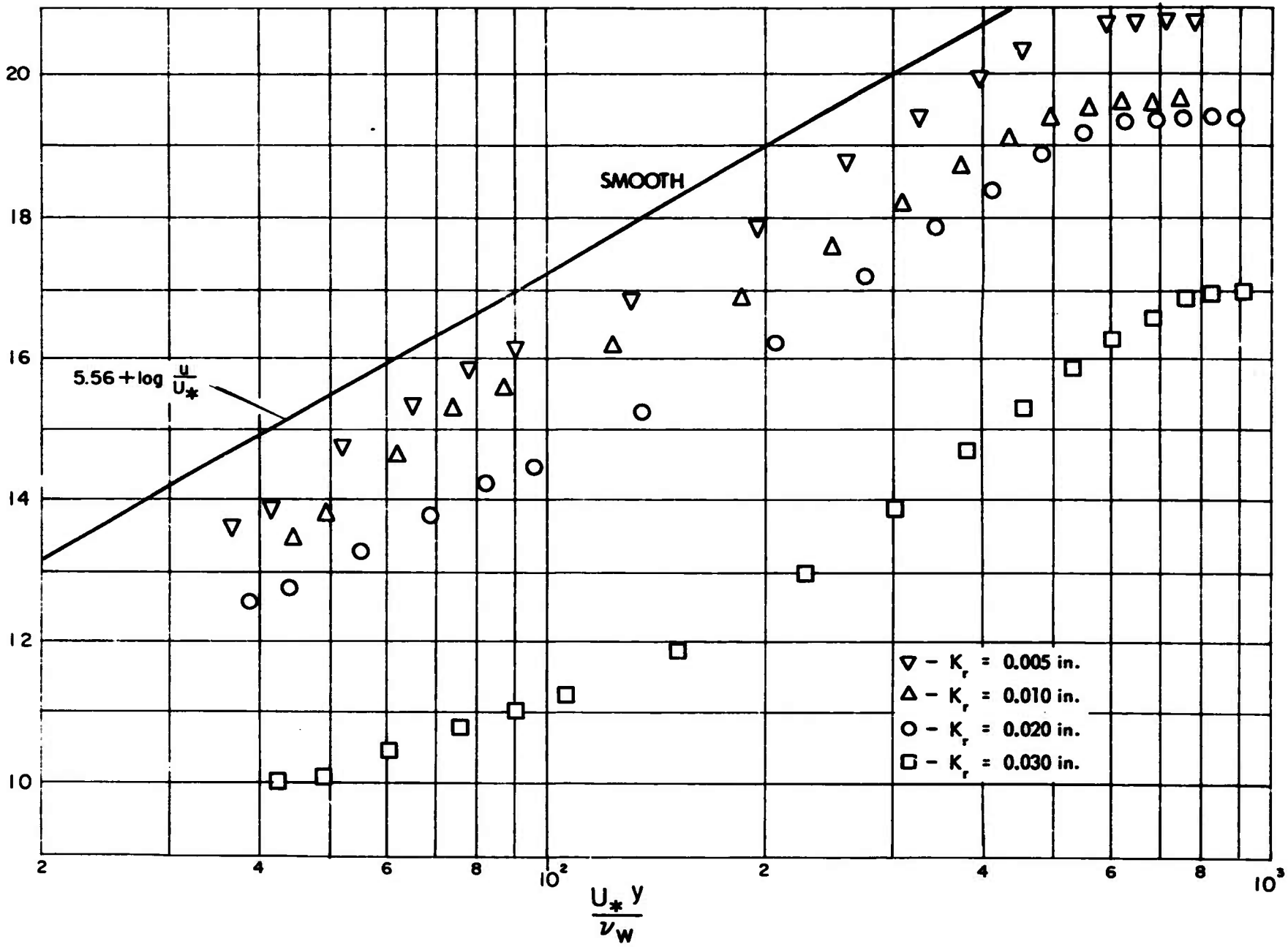

FIGURE 21
EXPERIMENTAL NONDIMENSIONAL VELOCITY DISTRIBUTION
FOR SMOOTH AND ROUGH FLAT PLATES
AT $M_1 = 4.93$ AND $T_w/T_1 = 3.8$

REFERENCES

1. Schlichting, H., Boundary Layer Theory, 6th Ed. (McGraw-Hill Book Co., New York, 1968).

2. Schultz-Grunow, F., "Neues Reibungswiderstandsgesetz fur glatte Platten," Luftfahrtforschung 17(8), 1940. (See also NACA Technical Memorandum No. 986, and Ref. (1), Fig. 21.3.)

3. Coles, D., "The Law of the Wake in the Turbulent Boundary Layer," J. Fluid Mech. 1, Part 2 (July 1956).

4. Reynolds, W. C., "A Morphology of the Prediction Methods," Proceedings, Computation of Turbulent Boundary Layers, - AFOSR-IFP-Stanford Conference, Vol. I, Kline et al., ed. (August 1968) pp. 1-15.

5. Rotta, J. C., "Critical Review of Existing Methods for Calculating the Development of Turbulent Boundary Layers," from Fluid Mechanics of Internal Flow, G. Sovran, ed. (Elsevier Publishing Co., Amsterdam, 1967) pp. 80-109.

6. Von Kármán, Th., "The Problem of Resistance in Compressible Fluids," Fifth Congress of the Volta Foundation on High Velocity in Aviation, Rome, 30 September - 6 October 1935, Royal Academy of Italy.

7. Wilson, R. E., "Turbulent Boundary Layer Characteristics at Supersonic Speeds - Theory and Experiment," J. Aeron. Sci. 17(9) (September 1950). (See also "Characteristics of Turbulent Boundary Layer Flow over a Smooth Thermally Insulated Flat Plate at Supersonic Speeds," Defense Research Laboratory Report No. 301, CM-712, June 1952, Ph.D. Dissertation, The University of Texas, Austin, Texas, 1952.)

8. Fenter, F. W. and C. J. Stalmach, Jr., "The Measurement of Turbulent Boundary Layer Shear Stress by Means of Surface Impact Pressure Probes," J. Aeron. Sci. 25(12) 793-794. (See also "Experimental Investigation of the Surface Impact Pressure Probe Method of Measuring Local Skin Friction at Supersonic Speeds," Defense Research Laboratory Report No. 392, CM-878, The University of Texas, Austin, Texas, October 1957.)

9. Wilson, R. E., "Viscosity and Heat Transfer Effects," Handbook of Supersonic Aerodynamics, Sections 13 and 14, NAVORD Report No. 1488, Vol. 5, U. S. Government Printing Office, Washington, D. C. (August 1966).

10. Prandtl, L., and H. Schlichting, "Das Widerstandsgesetz rauher Platten," (Werft, Reederei, Hafen, 1-4, 1934). (See also Prandtl, L., Collected Works, II, pp. 648-662.)

11. Fenter, F. W., "The Turbulent Boundary Layer on Uniformly Rough Surfaces at Supersonic Speeds," Defense Research Laboratory Report No. 437, CM-941, The University of Texas, Austin, Texas (January 1960). (See also Ph.D. Dissertation in Aerospace Engineering, The University of Texas, Austin, Texas, January 1960.)

12. Young, F. L., "Experimental Investigation of the Effects of Surface Roughness on Compressible Turbulent Boundary Layer Skin Friction and Heat Transfer," Defense Research Laboratory Report No. 532, CR-21, The University of Texas, Austin, Texas (May 1965). (See also Ph.D. Dissertation in Aerospace Engineering, The University of Texas, Austin, Texas, May 1965.)

13. Van Driest, E. R., "Turbulent Boundary Layer in Compressible Fluids," J. Aeron. Sci. 18(3) (March 1951).

14. Spalding, D. B., and S. W. Chi, "The Drag of a Compressible Turbulent Boundary Layer on a Smooth Flat Plate with and without Heat Transfer," J. Fluid Mech. 18, Part 1 (January 1964).

15. Moody, L. F., "Friction Factors for Pipe Flow," Trans. ASME 66 671 (1944).

16. Clutter, D. W., "Charts for Determining Skin-Friction Coefficients on Smooth and Rough Flat Plates at Mach Numbers up to 5.0, with and without Heat Transfer," Report No. ES 29074, Douglas Aircraft Co., Inc., El Segundo, California (April 1959).

17. Liepmann, H. W., and F. E. Goddard, Jr., "Note on the Mach Number Effect upon the Skin Friction of Rough Surfaces," J. Aeron. Sci. 24(10) 784 (October 1957).

18. Harkness, J. L., "The Effect of Heat Transfer on Turbulent Boundary Layer Skin Friction," Defense Research Laboratory Report No. 436, CM-940, The University of Texas, Austin, Texas (June 1959). (See also Ph.D. Dissertation, University of Texas, Austin, Texas, January 1959.)

19. Moore, D. R., "Velocity Similarity in the Compressible Turbulent Boundary Layer with Heat Transfer," Defense Research Laboratory Report No. 480, CM-1014, The University of Texas, Austin, Texas (April 1962). (See also Ph.D. Dissertation, The University of Texas, June 1962.)

20. Kempf, G., "Neue Ergebnisse der Widerstandsforschung," (Werft, Reederei, Hafen, 1929) Vol. 10, pp. 234-237.

21. Liepmann, H. W., and S. Dhawan, "Direct Measurements of Local Skin Friction in Low-speed and High-speed Flow," Proceedings of the First U. S. National Congress for Applied Mechanics, 869 (1951).

22. Hartwig, W. H., and J. E. Weiler, "The Direct Determination of Local Skin Friction Coefficients," Defense Research Laboratory Report No. 295, CF-1747, The University of Texas, Austin, Texas (January 1952).

23. O'Donnell, F. B., "A Study of the Effect of Floating-Element Misalignment on Skin-Friction-Balance Accuracy," Defense Research Laboratory Report No. 515, CR-10, The University of Texas, Austin Texas (March 1964). (See also Master's Thesis in Aerospace Engineering, The University of Texas, Austin, Texas, May 1964.)

24. Westkaemper, J. C., and F. B. O'Donnell, "Measurement Errors Caused by Misalignment of Floating-Element Skin-Friction Balances," AIAA Journal 2(1) (January 1965).

25. Preston, J. H., "The Determination of Turbulent Skin Friction by Means of Surface Pitot Tubes," J. Roy. Aeron. Soc. 58(110) (February 1954).

26. Hsu, E. Y., "The Measurement of Local Turbulent Skin Friction by Means of Surface Pitot Tubes," Report No. 957, David Taylor Model Basin, Washington, D. C. (August 1955).

27. Thompson, M. J., and J. F. Naleid, "Pressure Gradient Effects on the Preston Tube in Supersonic Flow," J. Aeron. Sci. 28(12) (December 1961). (See also Defense Research Laboratory Report No. 432, CF-2739, The University of Texas, Austin, Texas, and Master's Thesis in Aerospace Engineering, The University of Texas, Austin, Texas (August 1958).

REFERENCES (Cont'd)

28. Hill, O., "Experimental Investigation of the Impact Probe Method for Determining Local Skin Friction in the Presence of an Adverse Pressure Gradient for a Range of Mach Numbers from 1.70 to 2.75", Defense Research Laboratory Report No. 498, CF-3010, The University of Texas, Austin, Texas (January 1963). (See also Master's Thesis in Aerospace Engineering, The University of Texas, Austin, Texas, January 1963.)

29. Shutts, W. H., and F. W. Fenter, "Turbulent Boundary Layer and Skin Friction Measurements on an Artificially Roughened, Thermally Insulated Flat Plate at Supersonic Speeds," Defense Research Laboratory Report No. 366, CM-837, The University of Texas, Austin, Texas (August 1955).

30. Mann, H. W., "Experimental Study of the Compressible Turbulent Boundary Layer Skin Friction and Heat Transfer in the Fully Rough Regime," Defense Research Laboratory Report No. 554, The University of Texas at Austin (January 1968). (See also Master's Thesis in Aerospace Engineering, The University of Texas at Austin (August 1967).

31. Young, F. L., and J. C. Westkaemper, "Experimentally Determined Reynolds Analogy Factors for Flat Plates," AIAA Journal 3(6), 1201-2 (1965).

32. Bertram, M. H., ed., "Compressible Turbulent Boundary Layers," NASA SP-216. Proceedings of the Symposium at Langley Research Center, Hampton, Virginia, 10-11 December 1968.